Earth and Planetary Science Letters 297 (2010) 341–354

Contents lists available at ScienceDirect

Earth and Planetary Science Letters

journal homepage: www.elsevier.com/locate/epsl

Frontiers

Mantle dynamics and seismic anisotropy

Maureen D. Long [a,*], Thorsten W. Becker [b]

[a] Department of Geology and Geophysics, Yale University, New Haven, CT, USA
[b] Department of Earth Sciences, University of Southern California, Los Angeles, CA, USA

ARTICLE INFO

Article history:
Received 1 April 2010
Received in revised form 26 May 2010
Accepted 23 June 2010
Available online 31 July 2010

Editor: A.W. Hofmann

Keywords:
seismic anisotropy
mantle flow
geodynamic modeling
shear wave splitting
surface wave analysis
mantle convection

ABSTRACT

Observations of seismic anisotropy yield some of the most direct constraints available on both past and present-day deformation in the Earth's mantle. Insight into the character of mantle flow can also be gained from the geodynamical modeling of mantle processes on both global and regional scales. We highlight recent progress toward understanding mantle flow from both observations and modeling and discuss outstanding problems and avenues for progress, particularly in the integration of seismological and geodynamical constraints to understand seismic anisotropy and the deformation that produces it. To first order, the predictions of upper mantle anisotropy made by global mantle circulation models match seismological observations well beneath the ocean basins, but the fit is poorer in regions of greater tectonic complexity, such as beneath continental interiors and within subduction systems. In many regions of the upper mantle, models of anisotropy derived from surface waves are seemingly inconsistent with shear wave splitting observations, which suggests that our understanding of complex anisotropic regions remains incomplete. Observations of anisotropy in the D" layer hold promise for improving our understanding of dynamic processes in the deep Earth but much progress remains to be made in characterizing anisotropic structure and relating it to the geometry of flow, geochemical heterogeneity, or phase transitions. Major outstanding problems related to understanding mantle anisotropy remain, particularly regarding the deformation and evolution of continents, the nature of the asthenosphere, subduction zone geodynamics, and the thermo-chemical state of the lowermost mantle. However, we expect that new seismological deployments and closer integration of observations with geodynamical models will yield rapid progress in these areas.

1. Introduction

Seismic anisotropy, or the dependence of seismic wave speeds on the propagation direction or polarization of the waves, has been observed in many regions of the Earth's interior, including the crust, the upper mantle, the transition zone, the D" layer, and the inner core. Most of the scientific interest in delineating and interpreting seismic anisotropy is driven by the link between deformational processes and anisotropic structure. Deformation in the Earth often leads to seismic anisotropy, either through the crystallographic or lattice preferred orientation (CPO, LPO) of anisotropic constituent minerals, or through the shape preferred orientation (SPO) of materials with distinct isotropic elastic properties, such as partial melt. Because of this link between deformation and anisotropy, the characterization of anisotropic structure can yield some of the most direct constraints available on dynamic processes in the Earth's interior (Fig. 1).

Elastic anisotropy manifests itself in the seismic wavefield in a variety of ways, and a range of seismological tools can be used to characterize anisotropy in the Earth's mantle. Perhaps the most popular technique is measurement of shear wave splitting, a phenomenon that is analogous to optical birefringence under polarized light. Shear wave splitting, often measured using *SKS* phases, is an unambiguous sign of anisotropy and the measurement procedure itself is relatively straightforward, although the interpretation of splitting measurements (particularly in the context of complex anisotropic structure) is often complicated. Seismic anisotropy in the upper part of the mantle also manifests itself for surface waves. Differences in propagation speed between surface waves that are polarized differently (Rayleigh waves vs. Love waves) contain information about radial anisotropy, while the dependence of Rayleigh (or Love) wave velocities upon propagation direction contains information about azimuthal anisotropy, or the variation of seismic velocities within a horizontal plane. The free oscillations of the Earth excited by large earthquakes also contain information about anisotropy; different normal modes are sensitive to anisotropy in different depth ranges, and normal mode splitting can be measured and inverted to obtain anisotropic models of mantle and core structure.

In addition to the observational constraints obtained from seismological studies, insight into the pattern of mantle flow can be gleaned from geodynamical modeling, both in the laboratory and (more commonly) using numerical techniques. If the equations that govern solid-state flow are solved with appropriate boundary conditions, rheology and internal density anomalies, we can predict mantle circulation. Both global models and those that focus on a particular tectonic setting (e.g., subduction

* Corresponding author. Tel.: +1 203 432 5031.
E-mail address: maureen.long@yale.edu (M.D. Long).

0012-821X/$ – see front matter © 2010 Elsevier B.V. All rights reserved.
doi:10.1016/j.epsl.2010.06.036

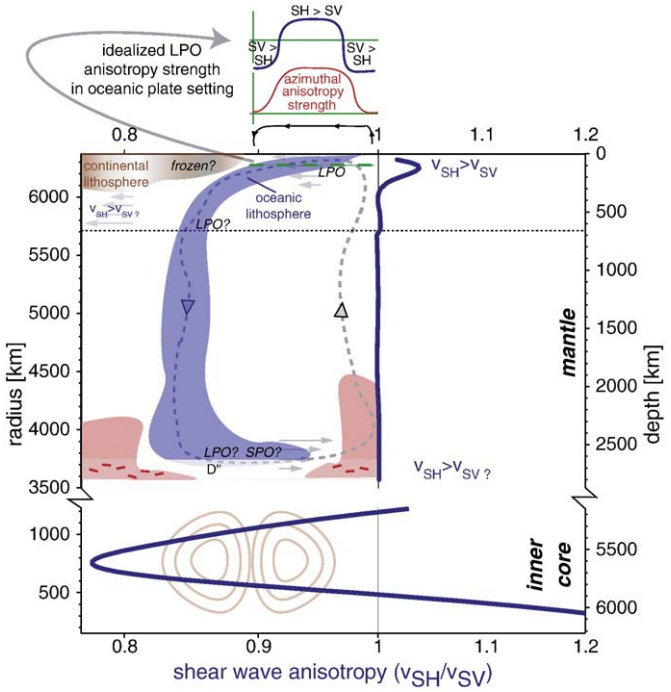

Fig. 1. Cartoon of the first-order anisotropic structure of the Earth (note the scale break at 2900 km depth, dotted horizontal line indicates the base of the transition zone at 660 km) with possible geodynamic interpretations. Heavy blue lines in the center show average radial anisotropy from Kustowski et al. (2008) for the mantle and from Beghein and Trampert (2003) for the inner core. The striking depth variation in inner core anisotropy is beyond the subject of this review, but is discussed in Beghein and Trampert (2003). Some possible radial and azimuthal anisotropy distributions from both active and fossil mantle deformation beneath continental regions and ocean basins are shown (cf. Montagner, 2007). The dashed line indicates a hypothetical flow trajectory for a downwelling slab (blue) displacing a thermo-chemical "pile" (red) at the core mantle boundary (cf. Garnero and McNamara, 2008) resulting in upgoing return flow. Beneath continental regions, both frozen-in anisotropy from past deformational episodes and sub-lithospheric anisotropy from active horizontal flow are likely present. Beneath ocean basins, mantle flow is likely primarily horizontal, leading to $V_{SH}>V_{SV}$, while the primarily vertical flow associated with possible upwellings and downwellings may lead to $V_{SV}>V_{SH}$. At the base of the mantle, possible horizontal flow due to slab material impinging upon the CMB is shown, which may lead to LPO and/or SPO anisotropy.

zones) are in use and yield complementary insights. Anisotropy provides a key observable that ties the predictions of geodynamics to seismology, and this is one of the more powerful methods of validating tectonic models. Joint interpretation allows inferences on global and regional plate dynamics, addressing questions such as the type and origin of plate motions, the role of mantle rheology, and causes and consequences of trench rollback.

Because of the intricacies of the link between flow and LPO or CPO anisotropy, the study of anisotropy as a marker for mantle deformation needs to be interdisciplinary. Our ability to interpret seismic anisotropy depends on the integration of geodynamical modeling and seismological observations via constraints from experimental mineral physics and observations of natural rocks derived from the mantle. The relationship between deformation and LPO anisotropy depends on the pressure, temperature, deviatoric stress, melt fraction, and water content under which the rocks are deformed. Detailed knowledge of the micromechanics of LPO formation appears therefore essential in order to fully link flow predictions to observations. Here, however, we focus on geodynamical modeling with simplified LPO treatment and comparisons with seismological observations. As a tool for deciphering the first-order controls on mantle flow, this approach has generally been successful.

In this review, we focus on anisotropy in the upper mantle (due to fossil deformation in the lithosphere and active flow in the asthenosphere) and in the D" layer just above the core–mantle boundary (CMB). Our intent is not to comprehensively cover every aspect of the diverse topic of seismic anisotropy, but rather to provide an overview of what we view as exciting research directions and major outstanding problems, with an emphasis on the recent literature. Our focus is on the integration of seismological observations and geodynamical modeling to ultimately answer first-order questions including the dynamics of subduction systems, the evolution of the continental lithosphere, the interactions between slabs, plates, and continental keels for tectonic motions, and the processes occurring in the D" region.

2. Sidebar I: jargon box

Seismic anisotropy is an intrinsic property of elastic materials that gives rise to the directional dependence of seismic wave speeds and particle motion polarizations, as well as the splitting of normal modes. Anisotropy is described mathematically by the *elasticity tensor*, which relates stress and strain in linearly elastic solids. For the most general form of anisotropy, 21 *elastic constants* are needed to describe the medium, but the Earth's mantle is often approximated with *hexagonal* or *transversely isotropic* symmetry, which requires 5 independent constants and specification of the orientation of the symmetry axis. Special classes of anisotropic geometry relevant for the Earth's mantle include *radial anisotropy,* which refers to a difference in propagation speed between horizontally and vertically polarized waves, and *azimuthal anisotropy*, which refers to a directional dependence of wave speed with azimuth. Anisotropy can be probed using *body waves* that propagate through the Earth's volume or *surface waves* that propagate along the surface and, in the case of fundamental modes, are sensitive to structure in the top few hundred kilometers of the mantle. *Rayleigh waves* are surface waves that involve elliptical, retrograde particle motion parallel to the direction of propagation and are mainly sensitive to the velocity of vertically polarized shear waves (V_{SV}); *Love waves* involve particle motion perpendicular to the propagation direction and are mainly sensitive to the velocity of horizontally polarized shear waves (V_{SH}). Shear body waves that propagate through an anisotropic medium undergo *shear wave splitting* into orthogonally polarized fast and slow components. *SKS phases* are a type of body wave that are commonly used in splitting studies; they are converted from a compressional wave to a shear wave at the *core–mantle boundary* (CMB) and therefore the polarization of the wave before it undergoes splitting is known. Other shear phases, such as *direct S*, are also used in splitting studies, and phases such as *ScS* (a shear wave that reflects off the CMB) and S_{diff} (a shear wave that is diffracted around the CMB) are used to probe anisotropy in D". Anisotropy in the mantle is often a consequence of *crystallographic* or *lattice preferred orientation* (CPO or LPO), which refers to non-random distributions of the orientations of individually anisotropic mineral grains in mantle rock and is also referred to as *fabric* or *texture*. *Olivine*, the primary upper mantle mineral constituent, has an intrinsic single-crystal shear wave anisotropy of ~18% and olivine LPO makes the largest contribution to upper mantle anisotropy, with *orthopyroxene* making a smaller contribution. In the deeper mantle, other minerals may contribute to anisotropy, including *perovskite*, *post-perovskite*, and *ferropericlase* in the lowermost mantle. Anisotropic structure can also be produced by *shape preferred orientation* (*SPO*), which is associated with the alignment of material with distinct isotropic elastic properties (contrasting with the surrounding matrix), such as melt pockets, or cracks in the shallowest crust.

3. The tools: seismology, mineral physics, and geodynamics

3.1. Seismological observations

A wide variety of seismological observables exist that can be used to infer anisotropic structure within the Earth. The main methods for characterizing mantle anisotropy are shear wave splitting and (for the upper mantle and transition zone) surface wave analysis, on which we focus here. However, several other seismological methodologies for

characterizing anisotropy exist. These include polarization analysis of long-period *P* waves (Schulte-Pelkum et al., 2001) and the analysis of *P* traveltime residuals for the asthenosphere (e.g., Bokelmann, 2002) and the deep mantle (e.g., Boschi and Dziewonski, 2000); for the upper mantle, these are often analyzed in combination with shear wave splitting (e.g., Plomerová et al., 1996). Azimuthal variations in *Pn* traveltimes can also be used to detect uppermost mantle anisotropy (e.g., Smith and Ekström, 1999) and anisotropic receiver function analysis yields information about sharp contrasts in anisotropic structure in the crust and uppermost mantle (Levin and Park, 1998). In addition to these body wave methods, analysis of the Earth's free oscillations can yield information about anisotropic structure in different regions, as different normal modes are sensitive to anisotropy in different depth ranges. Normal mode observations have been used to infer anisotropy in the inner core (e.g., Woodhouse et al., 1986; Beghein and Trampert, 2003) and, often in combination with surface wave measurements, in the mantle (e.g., Panning and Romanowicz, 2006).

Analysis of the splitting or birefringence of shear waves is perhaps the most popular method for studying anisotropy. Reviews of shear wave splitting methodologies and results can be found in Silver (1996), Savage (1999), and Long and Silver (2009a); here we provide a brief overview. A shear wave splitting measurement relies on the observation that when a shear wave with an initial linear polarization enters an anisotropic medium, it is split into two orthogonal components, one of which is oriented parallel to the fast direction of the anisotropic medium (Fig. 2).

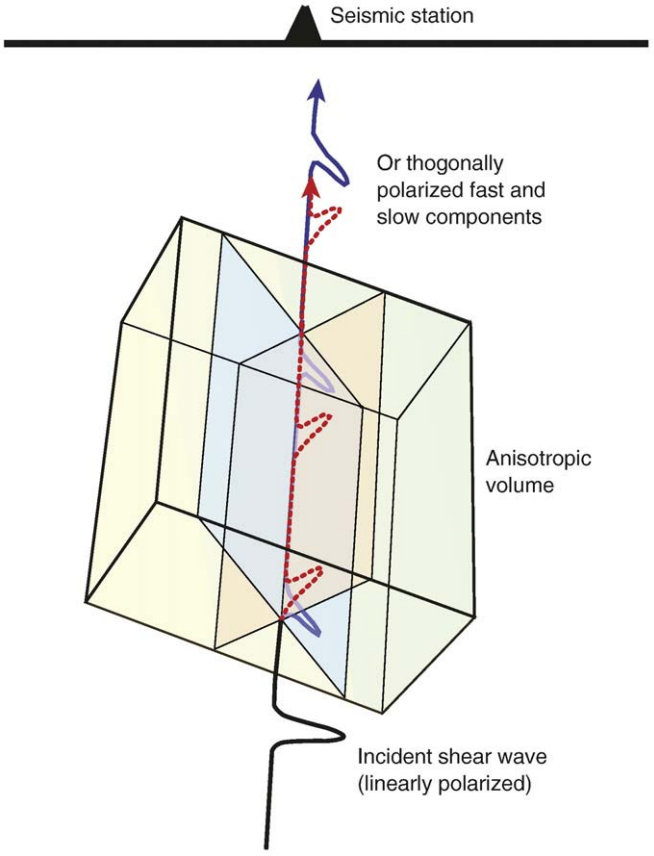

Fig. 2. Schematic diagram of shear wave splitting due to upper mantle anisotropy, after Garnero (http://garnero.asu.edu/research_images) and Crampin (1981). An incident, nearly vertical shear wave has an initial linear polarization before it hits the anisotropic volume (box). The shear wave splits into two components, one polarized parallel to the fast direction of the medium (blue) and one with orthogonal polarization (red). As the wave continues to propagate through the anisotropic medium, the components accumulate a time delay. The shear wave splitting parameters ϕ, which correspond to the azimuth of the fast component, and δt, the time delay between the fast and slow components, are measured directly from the seismogram.

As the two quasi-*S* waves propagate through the anisotropic region at different speeds, they accumulate a time delay. The orientation of the fast polarization direction, ϕ, and the delay time, δt, contain information about the geometry and the strength, respectively, of the anisotropic structure. Splitting measurement methods (e.g., Vinnik et al., 1989; Silver and Chan, 1991; Chevrot, 2000) are applied to a variety of shear phases that propagate through the mantle, including (most commonly) *SKS* and direct *S* at both local and teleseismic (that is, epicentral distances greater than ~40°) distances. *SKS* is particularly well suited to studying upper mantle anisotropy, as its initial polarization (before encountering the upper mantle on the receiver side) is controlled by the *P*-to-*S* conversion at the core–mantle boundary and is well known. Phases such as *SKS* and direct teleseismic *S* propagate nearly vertically through the upper mantle, and the measured fast direction ϕ reflects (approximately) the azimuth of fast wave propagation in the horizontal plane (azimuthal anisotropy).

Shear wave splitting has the advantage over other methods for characterizing anisotropy in that it is unaffected by isotropic wave speed heterogeneity and is therefore an unambiguous indicator of anisotropy. Splitting measurements also feature excellent lateral (on the order of half a Fresnel zone width, ~50 km) resolution, but because they are path-integrated measurements, the depth resolution of splitting measurements is poor. Arguments based on mineral physics considerations and comparisons between *SKS* and deep local *S* phases (e.g., Meade et al., 1995; Fischer and Wiens, 1996) suggest that *SKS* splitting generally reflects anisotropy in the upper mantle beneath the receiver, but an *SKS* measurement in isolation cannot place firm constraints on the depth distribution of anisotropy. Shear wave splitting observations often exhibit complexities that are inconsistent with a single homogeneous layer of anisotropy with a horizontal symmetry axis, which complicates the physical interpretation of splitting parameters. An example is the variation in measured splitting parameters with the initial polarization angle of the wave; in the presence of such variations, the measurements are known as "apparent" splitting parameters and cannot be simply related to the geometry of the anisotropy. When complex anisotropy is present, such complications in the splitting patterns must be accounted for, or the interpretation in terms of mantle flow may be misleading.

The analysis of surface wave propagation is a powerful complement to shear wave splitting (e.g., Montagner, 2007). Differences in propagation speed between horizontally and vertically polarized surface waves shed light on radial anisotropy in the upper mantle; this type of anisotropy can be probed by comparing the propagation of Love waves, which are primarily sensitive to V_{SH}, with that of Rayleigh waves, which are primarily sensitive to V_{SV}. Surface waves are dispersive, and different period phase velocities have peak sensitivities at different depths. This can be exploited to construct 3D models of anisotropy. Fundamental mode surface waves are sensitive to anisotropy in the uppermost few hundred kilometers of the mantle (e.g., Montagner and Nataf, 1986), while measurements of surface wave overtones are sensitive to structure as deep as the transition zone and the upper part of the lower mantle (e.g., Visser et al., 2008). Radial anisotropy deduced from surface waves is incorporated into both one-dimensional reference Earth models (e.g., Dziewonski and Anderson, 1981) and into 3D seismic tomography (e.g., Nataf et al., 1984; Panning and Romanowicz, 2006; Kustowski et al., 2008). Information about azimuthal anisotropy can also be extracted from the variation in Rayleigh wave speed on global (e.g., Montagner and Tanimoto, 1991; Debayle et al., 2005; Lebedev and van der Hilst, 2008) and regional (e.g., Forsyth, 1975; Simons et al., 2002; Deschamps et al., 2008) scales. Lateral gradients in anisotropy can give rise to Love-to-Rayleigh scattering, and the observation of so-called quasi-Love waves that have undergone this scattering can also yield constraints on upper mantle anisotropy (e.g., Rieger and Park, 2010). The signature of anisotropy in surface wave measurements can trade off with that of isotropic heterogeneity. However, the constraints on the depth dependence of anisotropy from surface waves provide an enormous

advantage over splitting measurements that lack depth resolution. Yet, surface waves have significantly poorer lateral resolution than splitting.

3.2. Mineral physics constraints

In order to relate anisotropic structure to flow geometry and processes in the mantle, it is crucial to understand the causative link between deformation and anisotropy. In most parts of the mantle, it is thought that LPO of intrinsically anisotropic minerals is the primary source of anisotropy, although SPO of melt or other materials may contribute to anisotropy in parts of the shallowest mantle (e.g., Greve and Savage, 2009) or in the D" region (e.g., Moore et al., 2004). Constraints on the relationship between deformation and LPO come mainly from laboratory experiments (e.g., Zhang and Karato, 1995; Bystricky et al., 2000; Jung et al., 2006) and, for the upper mantle, from the petrographic examination of mantle-derived rocks (e.g., Nicolas et al., 1971; Ben Ismaïl and Mainprice, 1998; Mehl et al., 2003; Mizukami et al., 2004; Skemer et al., 2006; Warren et al., 2008). Mineral and rock physics investigations into the formation of LPO form a large body of ongoing research, and we refer the reader to recent reviews by Mainprice (2007) and Karato et al. (2008).

In the upper mantle, olivine is volumetrically the most important mineral and because it has a large single-crystal anisotropy (~18% for shear waves; e.g., Mainprice, 2007), it is thought to make the primary contribution to the observed anisotropy. When an aggregate of olivine is deformed in simple shear in the dislocation creep regime, it will develop an LPO, with the strength of LPO increasing with increasing strain until it saturates at a relatively modest amount of strain (~100–150%, e.g., Karato et al., 2008). LPO patterns measured from most natural peridotites and in many laboratory experiments tend to suggest a fairly simple relationship: the maximum concentration of fast axes tends to align with the direction of maximum shear (see Fig. 3), which may be inferred from mantle flow models. As discussed in Section 5.2, when this type of LPO formation is used to relate strain and anisotropy, predictions from global models of mantle flow generally match seismological observations well, particularly in simple tectonic settings such as beneath the ocean basins. However, recent work on both laboratory and natural samples has revealed that the formation of LPO in olivine aggregates is more complicated than previously thought. In addition to the LPO pattern found in early simple shear experiments (e.g., Zhang and Karato, 1995), known as A-type, many other types of olivine fabric have been identified, including B-, C-, D-, and E-type (see Sidebar II for additional details). When olivine is deformed at relatively high stresses and low temperatures in the presence of water, B-type fabric dominates and in this case the fast axes of olivine tend to align 90° away from the maximum shear direction in the shear plane (Jung and Karato, 2001) (Fig. 3). Experimental work has shown that olivine fabric depends strongly on the conditions of deformation, including stress, temperature, and water content (e.g., Jung et al., 2006) and possibly pressure (e.g., Mainprice et al., 2005; Jung et al., 2009), although there has been some debate about the relative roles of pressure, stress, and water content in controlling LPO in some studies that have claimed evidence for a pressure-induced fabric transition (see Karato et al., 2008). While the details of the olivine "fabric diagram" in stress, temperature, water content, and pressure space are still being investigated, the dependence of olivine LPO geometry on deformation conditions presents both a challenge and an opportunity for seismological and modeling studies of upper mantle anisotropy. If anisotropy in the mantle can be illuminated in enough detail, then geodynamical models can be used to infer the olivine fabric type as a function of the prevailing temperature, stress, and water content conditions in the upper mantle (e.g., Karato, 2008; Becker et al., 2008).

While a great deal of work has been done on the olivine fabric diagram, much less is known about LPO formation in lowermost mantle materials; this is mainly due to the difficulties involved in performing deformation experiments at the pressures associated with the deeper

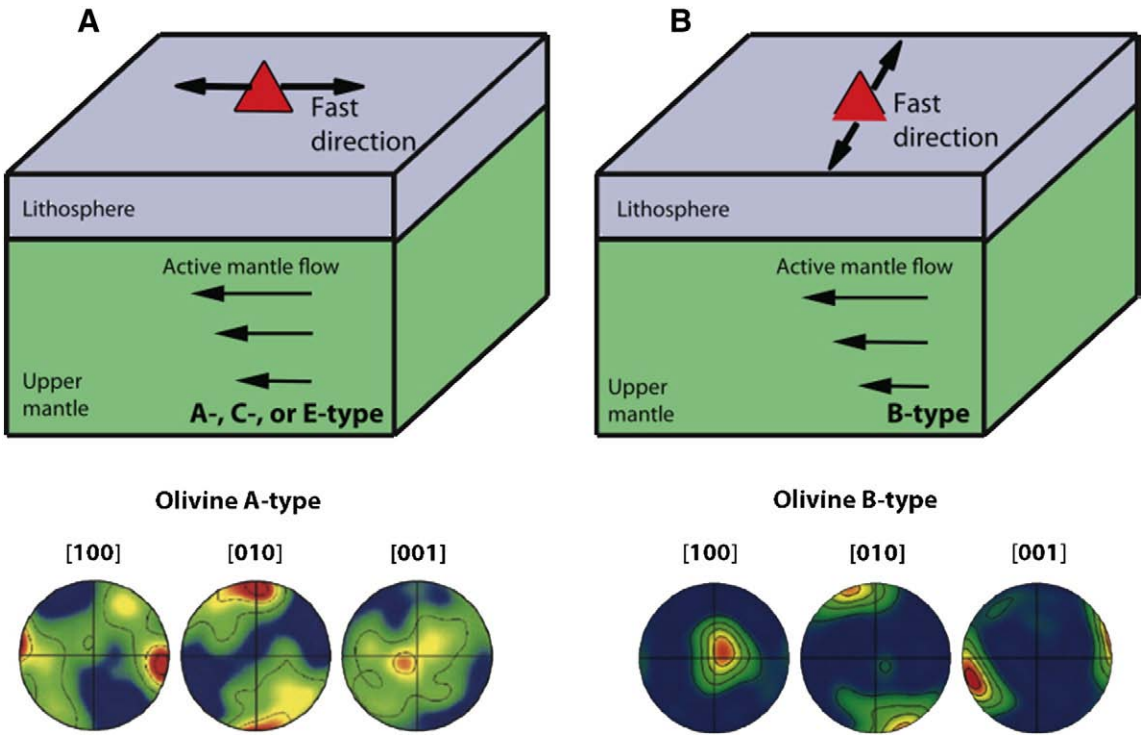

Fig. 3. Schematic diagram of the relationship between horizontal mantle flow and the resulting azimuthal anisotropy for different olivine fabric types. (A) In most regions of the asthenosphere, olivine fabric is expected to be A-, C-, or E-type, which would result in a fast axis of anisotropy that is parallel to the (horizontal) flow direction beneath a seismic station. Typical examples of pole figures for experimentally deformed olivine aggregates for A-type fabric are shown; the statistical distribution of the [100], [010], and [001] crystallographic axes are shown with respect to the deformation geometry (the horizontal line represents the shear plane). (B) If B-type olivine fabric, rather than A-, C-, or E-type, dominates, then the same flow direction would result in an observed fast direction that is different by 90°. Typical pole figures for B-type olivine are shown. All pole figures are from Karato et al. (2008), after Jung et al. (2006).

parts of the mantle (for a recent review, see Yamazaki and Karato, 2007). Most work has focused on understanding LPO development in ferropericlase (Mg,Fe)O, which has very high intrinsic anisotropy at D" pressures but which makes up only ~20–25% of the lowermost mantle by volume, and in the recently discovered post-perovskite phase (e.g., Yamazaki et al., 2006). There is still much debate about the dominant slip system in $MgSiO_3$ post-perovskite at the base of the mantle, as many of the relevant experiments have been carried out on analog materials (e.g., Yamazaki et al., 2006; Merkel et al., 2006) or at ambient temperatures (e.g., Merkel et al., 2007); particularly for low temperature experiments, their applicability to D" conditions is uncertain. It has been argued that predictions of D" anisotropy from experimentally determined LPO patterns match the first-order observations for both ferropericlase (e.g., Long et al., 2006) and post-perovskite (e.g., Wookey and Kendall, 2007), but both phases may play a role in controlling lowermost mantle anisotropy (Yamazaki and Karato, 2007) and D" anisotropy may well be controlled by the SPO of melt or slab graveyard materials (Kendall and Silver, 1998) rather than LPO.

3.3. Geodynamical models

The long-term deformation of the lithosphere and the convective motions of the mantle are governed by highly viscous, creeping flow of rocks in the laminar regime where inertial forces are negligible. The corresponding conservation of momentum (Stokes) equation has an instantaneous solution given mechanical boundary conditions, internal density anomalies, and rock viscosity. If viscosity is assumed to vary only with depth, semi-analytical solutions can be used to compute global circulation models for the mantle in spherical geometry. Surface boundary conditions can be plate motions (e.g., Hager and O'Connell, 1981), internal density anomalies may be estimated by scaling velocity anomalies from seismic tomography (e.g., Hager and Clayton, 1989), and viscosity profiles may be inferred from glacial isostatic adjustment and geoid anomalies (e.g., Hager, 1984). Such global circulation models (e.g., Fig. 4) can successfully explain a range of dynamic observables such as plate motions (e.g., Ricard and Vigny, 1989) and a recent review is given by Forte (2007). Lateral viscosity variations are expected to be of importance particularly for the upper mantle, and those require either iterative, spectral solutions (e.g., Zhang and Christensen, 1993) or fully numerical approaches (e.g., Zhong et al., 2000, 2007).

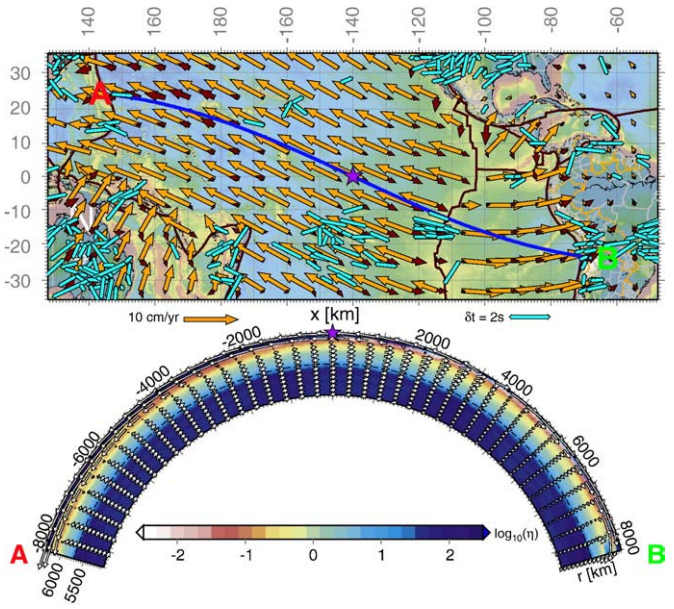

Fig. 4. Global circulation model predictions for a simple plate tectonic setting, across the Pacific. Both kinematic and density-driven flows are included in the model. Top: Profile location, surface velocities (orange vectors) and velocities at 230 km depth (dark red), as well as *SKS* splitting (cyan sticks, from a merged compilation after Fouch, 2006, and Wüstefeld et al., 2009, averaged on a $1^\circ \times 1^\circ$ grid). Bottom: Cross sectional velocities on top of model viscosity (normalized by 10^{21} Pas) down to 1300 km depth. Flow is from the best-fitting model from Becker et al. (2008, see that paper for details), as used in Fig. 5.

Assuming that surface boundary conditions are given by plate motions, the contribution to the deep mantle flow field that is not associated with return flow is proportional to the density anomalies, and inversely proportional to viscosity. Mineral physics provides some guidance on how to infer temperature from tomography, and flow models that use a simplified scaling relationship are successful in matching first-order observations of azimuthal and radial anisotropy (e.g., Gaboret et al., 2003; Becker et al., 2003, 2008; Behn et al., 2004; Conrad et al., 2007). However, there is always a complicating trade-off between temperature and composition as inferred from seismic velocity anomalies, particularly in cratonic regions and in the deep mantle (e.g., Simmons et al., 2009). From laboratory experiments, mantle viscosity is expected to depend not only on pressure, temperature, and composition but also on deviatoric stress, grain size, volatiles (e.g., water) and melt fraction (e.g., Kohlstedt, 2007), and flow will also depend on the deformation history in the case of mechanical anisotropy (e.g., Christensen, 1987; Chastel et al., 1993). Water, melt, grain size (via the partitioning between diffusion and dislocation creep) and stress level are all expected to affect LPO development, which will in turn control mechanical anisotropy, making the flow prediction problem inherently non-linear (e.g., Pouilloux et al., 2007; Lev and Hager, 2008a; Tommasi et al., 2009; Knoll et al., 2009). There are large rheological uncertainties involved, in terms of the appropriate creep law parameters and the distribution of relevant fields, such as volatiles, in the Earth. Such complexities motivate a step-wise approach where simplified geodynamic models that match first-order observations are progressively refined.

Global mantle flow may significantly modify regional velocities as inferred from local driving forces in settings such as subduction zones (e.g., Becker and Faccenna, 2009). However, at a given computer resource level, regional models can achieve higher numerical resolution and are better at representing smaller scale features, particularly in 3D. One approach is to "couple" regional, high resolution models with large-scale models (e.g., Tan et al., 2007; Mihalffy et al., 2008); others are to use variable mesh refinement, or to simply run global models at high resolution (~30 km scales can now be routinely resolved).

From mantle flow, LPO formation can be computed, either subsequently, if it is assumed that LPO does not feed back into rheology, or jointly while solving for mantle flow. LPO fabrics may be inferred by following strain-rates along advected particle paths and computing either finite strain orientations (e.g., McKenzie, 1979; Hall et al., 2000) or a more elaborate prediction of texture. Texturing microphysics approaches in use include visco-plastic self consistent theory (e.g., Wenk et al., 1991; Chastel et al., 1993; Blackman et al., 2002) and kinematic approximations (e.g., Kaminski and Ribe, 2001; Kaminski et al., 2004). LPO predictions between these models are broadly consistent with the exception of regions of rapid reworking of fabric (e.g., Castelnau et al., 2009), and outside such regions approximate methods such as the infinite strain axis (Kaminski and Ribe, 2002) may be sufficient to capture anisotropy (e.g., Conrad et al., 2007). Particularly if LPO is computed jointly with mantle flow, simplified methods for treating dynamic LPO generation such as directors may be advantageous and sufficiently precise (Lev and Hager, 2008b), although they may be inadequate when rapid spatial variations in flow geometry or fabric regime are present. Further constraints from the field and laboratory experiments on LPO reworking are required to resolve questions about the appropriate theoretical treatment of LPO. However, the kinematic description of LPO formation is able to capture different types of fabrics (Kaminski, 2002) and produces LPO heterogeneity similar to those seen in field samples

when employed in global mantle flow models (Becker et al., 2006), providing some *a posteriori* justification for the geodynamic models.

4. Sidebar II: olivine fabric types

Both experimental studies and examinations of mantle-derived rocks have revealed that olivine LPO is quite complex and a variety of olivine fabric types have been identified both in the laboratory and in nature, including A-, B-, C-, D-, and E-type fabrics (see, e.g., Mainprice, 2007; Karato et al., 2008). Early simple shear experiments on dry olivine aggregates done at modest stress and temperature revealed A-type fabric, which is associated with dominant slip in the [100] direction on the (010) plane. In this regime, the fast axes of individual olivine crystals tend to align in the direction of shear; for horizontal mantle flow, this would imply that the measured fast direction of azimuthal anisotropy should correspond to the horizontal flow direction. B-type fabric, which is associated with slip in the [001] direction on the (010) plane and is favored by high stresses, low temperatures, and some amount of water, changes this relationship by 90°. At high temperatures and low stresses, the dominant fabric type is expected to change from A-type to E-type ([100](001) slip dominates) to C-type ([001](100) slip dominates) with increasing water content. The possible effect of pressure on olivine fabric is controversial and is still being investigated experimentally. A-type or D-type fabric is expected to dominate in the mantle lithosphere, while C-, E-, or A-type fabric likely dominates in the asthenosphere. B-type fabric may be present in the cold corner of the subduction mantle wedge, where stresses are high and temperatures are low. For the case of horizontal flow in the upper mantle, all fabric types except for B-type would produce fast directions of azimuthal anisotropy that are parallel to the flow direction; for B-type, the fast direction would be normal to the flow direction (Fig. 3). For radial anisotropy, predictions for the same horizontal flow scenario are as follows: A-, B-, and D-type would predict relatively strong $V_{SH}>V_{SV}$ anisotropy, while E-type would predict weak $V_{SH}>V_{SV}$ and C-type would predict $V_{SV}>V_{SH}$. For a more detailed description of olivine fabrics and their seismological implications, we refer the reader to Mainprice (2007) and Karato et al. (2008), and references therein.

5. Anisotropy and mantle flow: global and regional observations and models

5.1. First-order anisotropic structure of the Earth

Using the methods described in Section 3.1, the first-order characteristics of anisotropy in the Earth's interior have been imaged (Figs. 1 and 5). Although not the subject of this review, we note that there is significant anisotropy in the crust (e.g., Mainprice and Nicolas, 1989; Weiss et al., 1999; Crampin and Chastin, 2003; Meissner et al., 2006) and there is also strong anisotropy in the inner core (e.g., Beghein and Trampert, 2003; Souriau, 2007). In the upper ~250 km of the mantle, on average up to ~4% radial anisotropy is present, with $V_{SH}>V_{SV}$ (that is, horizontally polarized shear waves traveling faster, in the horizontal plane, than vertically polarized ones). The strength of radial anisotropy in most models peaks at a depth of ~150 km; this may correspond to boundary-layer flow type deformation in the low-viscosity asthenosphere. The presence of radial anisotropy below the upper mantle is less well constrained (e.g., Boschi and Dziewonski, 2000; Panning and Romanowicz, 2006; Visser et al., 2008), in part due to the severe trade-offs between radial anisotropy and crustal structure in global surface wave tomographic inversions (e.g., Ferreira et al., 2010). There is some evidence for radial and/or azimuthal anisotropy in the transition zone (e.g., Trampert and van Heijst, 2002; Wookey and Kendall, 2004), but the bulk of the lower mantle generally appears to be isotropic (e.g., Meade et al., 1995) with the exception of the D" layer at the base of the mantle (e.g., Panning and Romanowicz, 2006; Wookey and Kendall, 2007). The observation of lower mantle isotropy would suggest that deformation is being accommodated by a process other than dislocation creep that does not produce LPO, such as diffusion creep or superplasticity (e.g., Karato et al., 1995). In contrast, the presence of anisotropy in D" would suggest either a transition to dislocation creep (e.g., McNamara et al., 2002) or the presence of SPO of elastically distinct material, such as partial melt (e.g., Kendall and Silver, 1998).

5.2. Global flow models and comparisons with upper mantle observations

Given the association of LPO anisotropy with plate tectonic motions (e.g., McKenzie, 1979), the link between global seismological models of azimuthal anisotropy (cf. Fig. 5A) and mantle flow has been made in a qualitative fashion early on (e.g., Tanimoto and Anderson, 1984). The simplest comparison is between azimuthal anisotropy and absolute plate motions in some reference frame (APM hypothesis), where the idea is that the mantle is being sheared such that fast velocity orientations of LPO anisotropy are aligned with plate motions. Global circulation models allow more refined estimates, and the example depicted in Fig. 4 shows that flow at asthenospheric depths, and hence relative shearing, will only in simple settings be aligned with surface velocities, such as in the center of the Pacific plate.

Gaboret et al. (2003) compared azimuthal anisotropy with stretching-rates from flow model predictions and found a good match for the

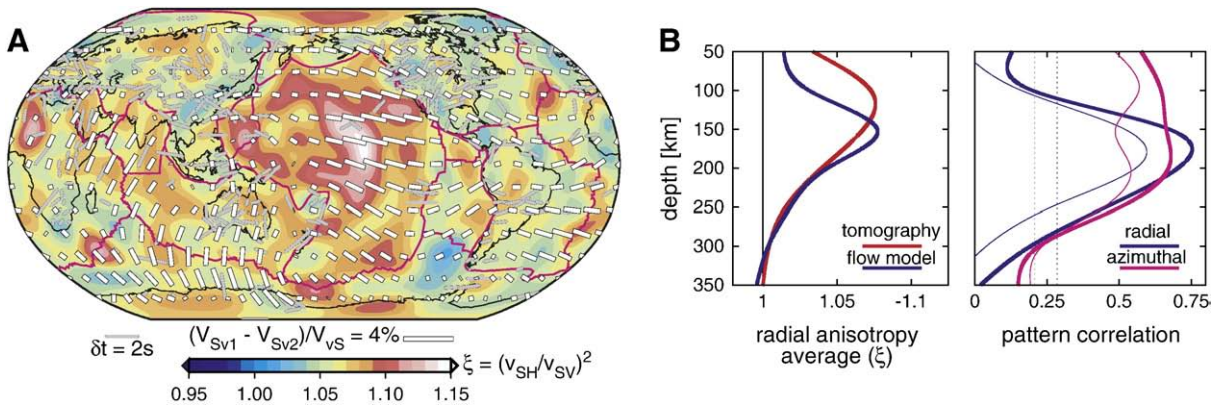

Fig. 5. Global uppermost mantle seismic anisotropy. (A) Radial (background, from Kustowski et al., 2008) and azimuthal (white sticks indicating fast orientation, from Lebedev and van der Hilst, 2008) anisotropies are from surface wave analysis, shown at 150 km depth along with *SKS* splitting (gray sticks, 5° × 5° averages of the compilation of Fig. 4). (B) Radial anisotropy layer averages (left panel, $\xi = (V_{SH}/V_{SV})^2$) and as predicted from the best-fitting geodynamic model of Becker et al. (2008) (velocities shown in Fig. 4). In the right panel, pattern correlations up to spherical harmonic degree 8 between the same geodynamic model and radial and azimuthal seismological models. Thin and heavy lines denote the global correlations and those for oceanic lithosphere only, respectively. Vertical dashed lines indicate the 95% significance level.

Pacific plate at asthenospheric (~150 km) depth. Becker et al. (2003) tested the alignment of finite strain orientations as inferred from particle trajectories (cf. Hall et al., 2000) for several global flow models against a set of surface wave phase velocity maps. Becker et al. (2003) showed that the flow estimates outperformed the simple APM model, and that circulation models that included active mantle flow did better than those which included plate motion associated currents only. Similarly, Behn et al. (2004) showed that *SKS* splitting in oceanic plates can be matched if active upwellings are included and used this as a constraint on absolute viscosity values, assuming that density structure is known from tomography. Becker et al. (2008) used LPO predictions as inferred from the kinematic approach of Kaminski et al. (2004) for A-type deformation (cf. Becker et al., 2006). They showed that radial anisotropy averages provide constraints on mantle rheology (the depth regions for dominance of dislocation creep, as a function of grain size), and that a single geodynamic model can be used to fit both azimuthal and radial anisotropy patterns (Fig. 5B).

The success of such flow models in matching observations in oceanic domains implies that the general view of convective formation of LPO anisotropy (Fig. 1) is correct, that circulation models provide reliable large-scale estimates of mantle flow, and that mineral physics theories based on laboratory results yield probable global LPO estimates. This also means that it is likely that A- or E-type LPOs are the dominant fabrics at asthenospheric depths; if the high pressure or high water content types of LPO were ubiquitous, the match to geodynamic flow predictions could not be as good.

Synthetic anisotropy from flow models may then be used as a geodynamic reference against which interesting second-order deviations can be tested. For radial anisotropy within the Pacific (Fig. 5A), for example, one may invoke lateral variability in the hydration state of the mantle (Karato, 2008). Allowing for small fractions of C-type in addition to A-type LPO in flow models (Becker et al., 2008) improves the match to anisotropy dramatically (as expected from the complementary predictions for A-type vs. C-type fabric); the inferred volatile variations are moderate and similar approaches may eventually allow "imaging" of global water distribution (cf. Lassak et al., 2006). Conrad et al. (2007) explored the role of lateral viscosity variations; allowing for those led to a slight improvement in fit to *SKS* splitting underneath continental domains. Another inference that is made possible by anisotropy synthetics includes tests for absolute plate motion reference frames. Becker (2008) showed that large net rotations of the lithosphere are incompatible with azimuthal anisotropy from surface waves; the latter impose a net rotation speed limit of ~50% of HS3 (Gripp and Gordon, 2002). Complementary modeling studies by Kreemer (2009) and Conrad and Behn (2010) that employ different approaches for comparisons with anisotropy (mainly utilizing *SKS* splitting) yield consistent conclusions.

5.3. Subcontinental anisotropy

An important complexity in the interpretation of upper mantle anisotropy arises in the continental lithosphere (Figs. 1 and 6) where dynamic models are less certain, and anisotropy is less consistently imaged than for oceanic domains (e.g., Fouch and Rondenay, 2006). As Fig. 5B shows, anisotropy patterns are less well matched in the continents (Becker et al., 2003; Conrad et al., 2007), and radial anisotropy averages are severely under-predicted. One hypothesis states that the strongest contribution to upper mantle anisotropy underneath continental plates is due to frozen-in structure. In fact, the geography of the regions and the amplitude by which the convective

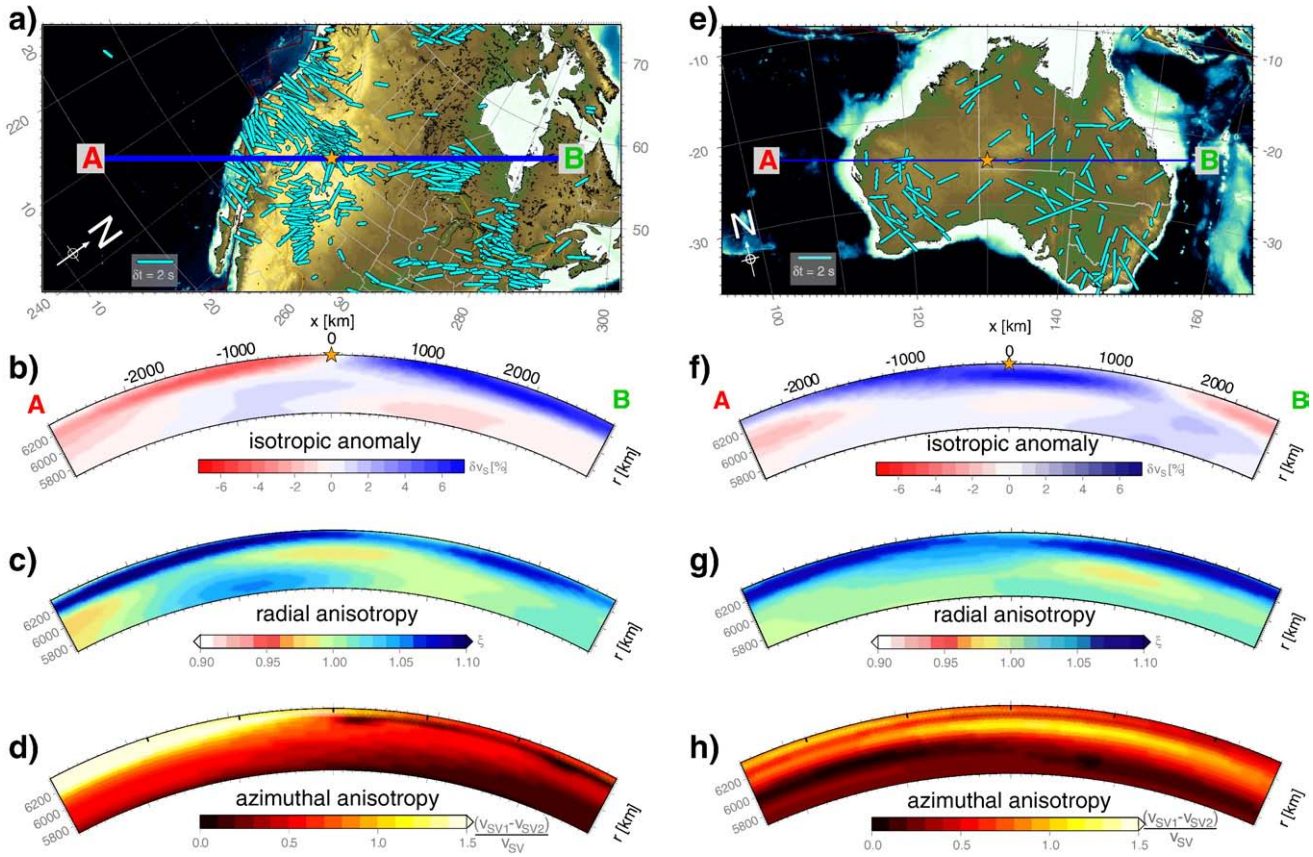

Fig. 6. A comparison of the observed anisotropic structure of the North American (a–d) and Australian (e–h) continents. Top panels show *SKS* splitting observations (cyan sticks) from the compilation of Fig. 4; the location of the cross sections shown in the lower panels is shown as a blue line. The lower panels show the strength of the isotropic shear wave speed anomaly (Voigt average, b and f), radial anisotropy (c and g), and azimuthal anisotropy (d and h, peak to trough). The isotropic and radially anisotropic structures are from Kustowski et al. (2008) and azimuthal anisotropy is from Lebedev and van der Hilst (2008).

anisotropy model of Becker et al. (2008) underpredicts radial anisotropy at shallow depths of 50 km are consistent with an origin due to frozen-in structure in cratonic regions, which can be explored by stochastic modeling (e.g., Becker et al., 2007).

It is far from clear, however, what the relative contributions are to the observed anisotropic signal from frozen anisotropic structure in the lithosphere versus contemporary flow in the asthenosphere in all continental regions (e.g., Deschamps et al., 2008). Shear wave splitting data in continental interiors are often complicated, exhibiting significant heterogeneity over short length scales (e.g., Fouch et al., 2004; Heintz and Kennett, 2005). Such heterogeneity would suggest a contribution from complex anisotropy in the shallow lithosphere, but because of the poor depth resolution of splitting measurements, the relative contributions of lithospheric and asthenospheric anisotropy are difficult to quantify. Surface wave analysis can provide depth constraints, but the coarse lateral resolution of surface wave tomography means that small-scale lateral variations in lithospheric anisotropy will not be well resolved. A comparison between North America and Australia (Fig. 6) serves to highlight poorly understood differences between the two cratonic regions: surface wave models of the upper mantle beneath Australia reveal strong azimuthal anisotropy at asthenospheric depths (e.g., Simons et al., 2002; Debayle et al., 2005; Lebedev and van der Hilst, 2008), but the shear wave splitting patterns exhibit little spatial coherence and observed delay times are often small (e.g., Clitheroe and van der Hilst, 1998; Heintz and Kennett, 2005, 2006). Conversely, relatively strong and coherent splitting is observed beneath the interior of the North American continent, which has been interpreted as evidence for shear in the asthenosphere driven by plate motion (Fouch et al., 2000), but global surface wave models (e.g., Lebedev and van der Hilst, 2008) do not show particularly strong azimuthal anisotropy beneath cratonic North America.

5.4. Mantle flow in subduction systems

Plates are mainly driven by slabs, and subduction zones represent some of the most tectonically complex and important settings on Earth. Most of the constraints on subduction zone mantle flow come from shear wave splitting measurements, as surface wave inversions typically lack the required lateral resolution. Because different parts of the subduction system, including the overriding plate, the mantle wedge, the slab, and the sub-slab mantle, likely contribute to the shear wave splitting, it is imperative to properly separate the different effects. This can be accomplished at least in part by considering raypaths that sample different regions of the subduction system, including local *S* phases from slab earthquakes that mainly sample the mantle wedge (e.g., Fischer and Wiens, 1996; Fischer et al., 2000; Levin et al., 2004; Long and van der Hilst, 2006; Pozgay et al., 2007; Abt et al., 2009) and source-side teleseismic *S* measurements from slab earthquakes that have been corrected for anisotropy beneath the receiver and mainly reflect sub-slab anisotropy (e.g., Russo and Silver, 1994; Russo, 2009) along with *SKS* (or teleseismic *S*) splitting measurements (e.g., Abt et al., 2010).

Fig. 7 shows a cartoon of shear wave splitting behavior observed in subduction zones worldwide, from the compilation of Long and Silver (2008, 2009b). The parts of the signal attributed to wedge and sub-wedge anisotropy (which could be in the slab and/or the sub-slab mantle) are shown separately. Several first-order characteristics are evident: beneath the wedge, fast directions are generally trench-parallel, which could be due to trench-parallel sub-slab mantle flow induced by trench migration (e.g., Russo and Silver, 1994; Long and Silver, 2008, 2009b) or due to serpentinized aligned cracks in the shallow slab (Faccenda et al., 2008). In the mantle wedge, fast directions are usually complex and often exhibit a characteristic change in orientation from trench-parallel close to the trench to trench-perpendicular in the backarc in many systems. This change in orientation has variously been interpreted as being due to the presence of B-type olivine or serpentinite fabric in the cold corner of the mantle wedge (e.g., Karato, 1995; Nakajima and Hasegawa, 2004; Lassak et al., 2006; Kneller et al., 2008; Katayama et al., 2009; Bezacier et al., 2010), the dominance of trench-parallel mantle wedge flow (e.g., Hall et al., 2000; Smith et al., 2001; Mehl et al., 2003; Kneller and van Keken, 2008; Hoernle et al., 2008), or complex 3D flow due to lower crustal foundering below the arc (Behn et al., 2007). A wide range of delay times are also observed for both the sub-wedge region and the wedge, with average δt values ranging from near isotropy up to ~1.5 s or more. While ambiguities about the interpretation of shear wave splitting measurements in terms of mantle flow in subduction settings remain, it is clear that the classical flow model for subduction

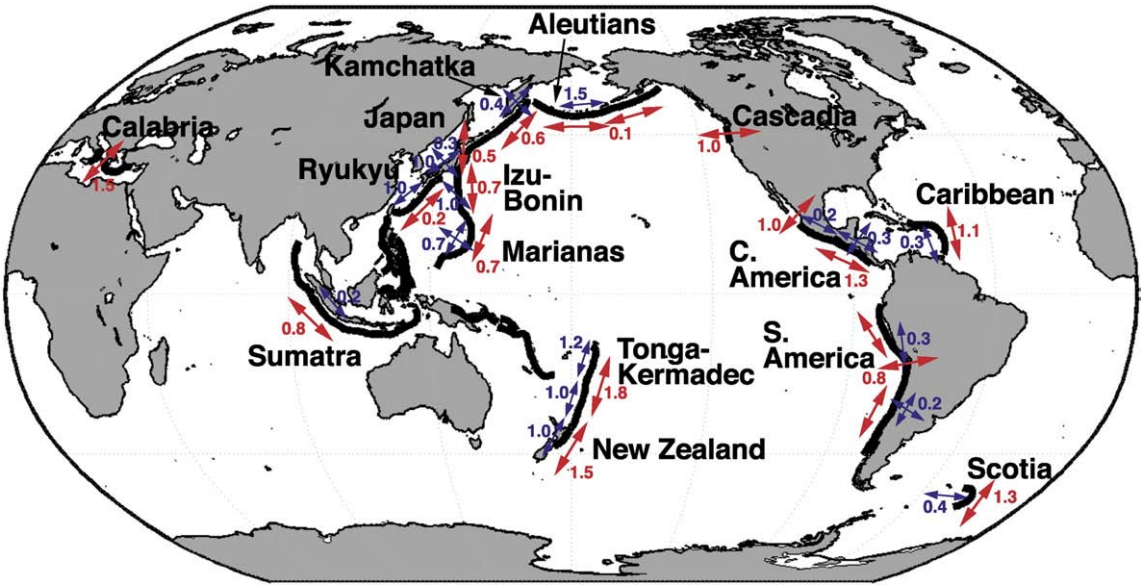

Fig. 7. Sketch of constraints on subduction zone anisotropy from shear wave splitting measurements from the compilation of Long and Silver (2008, 2009b). The anisotropic signals of the wedge and sub-slab regions are shown separately. Red arrows indicate average fast directions for the sub-slab splitting signal from *SKS*, local *S*, and source-side teleseismic *S* splitting measurements. The associated average sub-slab delay times are shown in red. Blue arrows indicate average fast directions for wedge anisotropy from local *S* splitting. In regions where multiple fast directions are shown, splitting patterns exhibit a mix of trench-parallel, trench-perpendicular, and oblique fast directions.

zones (two-dimensional corner flow above the slab and two-dimensional entrained flow beneath) fails to explain the diversity of observations in subduction zones globally.

In addition to constraints provided from shear wave splitting observations, insights about the character of mantle flow in subduction systems have been provided by geodynamic modeling (e.g., reviews by Billen, 2008; Becker and Faccenna, 2009). Many studies have explored the effects that two-dimensional corner flow in the wedge has on, for example, the thermal structure of subduction zones (e.g., Peacock, 2003; England and Wilkins, 2004) or the resulting shear wave splitting patterns at the surface (e.g., Fischer et al., 2000), also allowing for along-trench flow in a 2.5D framework (Hall et al., 2000), where there is no variation in the model in the third dimension. In 3D, the effect of complex slab morphology on the mantle flow patterns in the wedge has been explored by Kneller and van Keken (2008). Several have studied the importance of larger-scale 3D flow due to trench migration, both from a laboratory (e.g., Gouillou-Frottier et al., 1995; Kincaid and Griffiths, 2003; Funiciello et al., 2006) and a numerical modeling perspective (e.g., Piromallo et al., 2006; Stegman et al., 2006; Schellart et al., 2007). An example of such a model that highlights the role of 3D flow is shown in Fig. 8; the slab is allowed to retreat freely and this slab rollback induces strongly trench-parallel flow beneath the slab (Becker and Faccenna, 2009),

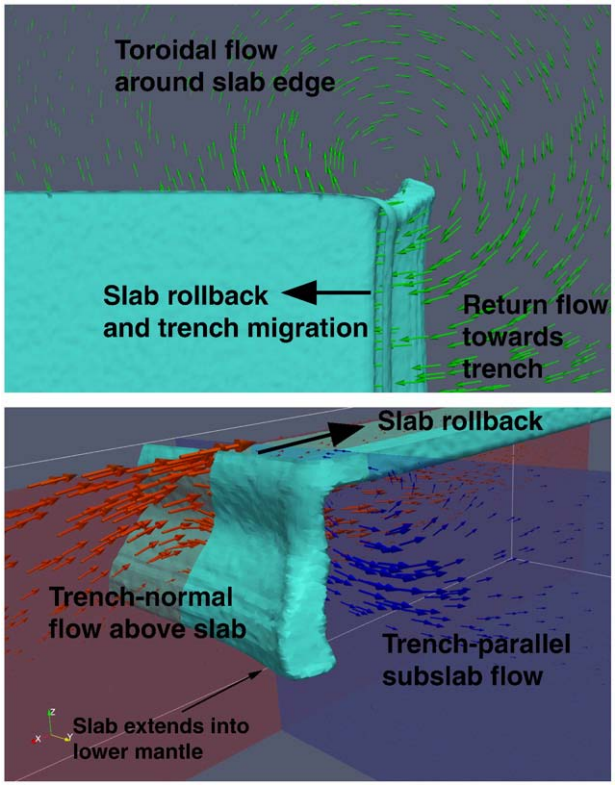

Fig. 8. An example of a regional, 3D subduction zone model, after Becker and Faccenna (2009). Shown is a snapshot from a fully dynamical computation in map (top) and oblique side view (bottom). The trench is rolling back (migrating to the left in the top figure), as induced by a dense, relatively stiff, viscous slab (shown in turquoise) that descends into the upper mantle and encounters a viscosity increase at 660 km. Green arrows (top) show the velocities in a horizontal plane and exhibit significant toroidal flow, with trench-perpendicular return flow toward the trench in the wedge above the central part of the slab, and some trench-parallel flow in the wedge in the vicinity of the slab edge. In the bottom figure, red and blue arrows show velocities in two vertical slices that are parallel and perpendicular, respectively, to the direction of trench migration. Only the in-plane components of the velocity vector are shown. Beneath the slab, there is a strong component of trench-parallel flow (blue arrows). Above the slab, flow is dominantly trench-normal (particularly in the central part of the slab) and is controlled by the trench migration.

similar to what is suggested by the model of Long and Silver (2009b). Many models that seek to explore subduction zone processes such as the production and migration of melt and volatiles through the mantle wedge use two-dimensional frameworks that do not address the possibility of trench-parallel flow (e.g., Cagnioncle et al., 2007; Grove et al., 2009). Given the likely presence of 3D, trench-parallel and toroidal flow in many (if not all) mantle wedge settings, along-strike flow should be further explored (cf. Hall et al., 2000; Kincaid and Griffiths, 2003; Zandt and Humphreys, 2008).

5.5. The D" region

Compared to the upper mantle, the study of anisotropy in the lowermost mantle is still in its infancy. Because of the insights that anisotropy can yield into dynamics, however, the delineation and interpretation of D" anisotropy hold great promise for increasing our understanding of the dynamics of the deep mantle. There is a large amount of observational evidence for anisotropy in the D" layer at the base of the mantle, in sharp contrast to the generally isotropic lower mantle above it. Several dozen shear wave splitting studies have identified D" anisotropy (e.g., Wookey and Kendall, 2007 and references therein), and global radially anisotropic mantle models also show significant anisotropy at the base of the mantle (e.g., Boschi and Dziewonski, 2000; Panning and Romanowicz, 2006). Most body wave studies utilize shear phases that propagate nearly horizontally through the D" layer, such as *S*, S_{diff}, and (at large epicentral distances) *ScS* (e.g., Ritsema, 2000; Garnero et al., 2004; Wookey et al., 2005; Wookey and Kendall, 2007), although discrepancies between *SKS* and *SKKS* splitting have also been interpreted in terms of anisotropy in the lowermost mantle (e.g., Long, 2009). D"-associated shear wave splitting is often characterized (after correcting the waveforms for splitting due to anisotropy near the receiver and/or the source) by measuring the traveltime difference between horizontally and vertically polarized shear components, and therefore reflects radial anisotropy, although azimuthal anisotropy has been inferred in some studies (e.g., Garnero et al., 2004; Long, 2009). In most regions, $V_{SH} > V_{SV}$ anisotropy appears to predominate, particularly in regions that are associated with relatively high isotropic *S* wave speeds (Wookey and Kendall, 2007), which suggests that this style of anisotropy may correspond to the presence of subducted slab material above the CMB (cf. Fig. 1). In some regions, however, such as the central and southeastern Pacific, anisotropy appears to be more variable, with some regions of $V_{SV} > V_{SH}$ and some regions that appear to be isotropic.

Although many regions of D" have not yet been studied with respect to their anisotropic structure, at this point a first-order picture of anisotropy at the base of the mantle has emerged. A framework for the interpretation of this picture in terms of dynamic processes, however, remains elusive. Both LPO- and SPO-based mechanisms have been proposed (e.g., Kendall and Silver, 1998; Karato, 1998), and since both types of mechanisms appear to explain the first-order features of D" anisotropy (e.g., Long et al., 2006), it is difficult to distinguish between the two observationally. Two scenarios for explaining D" anisotropy, one of which invokes LPO in the vicinity of a subducting slab and one of which invokes SPO in a region with partial melt, are shown in Fig. 9. The spatial correspondence between regions of $V_{SH} > V_{SV}$ and relatively high *S* wave speeds has also led to the suggestion that this anisotropic geometry may be associated with the presence of post-perovskite (e.g., Wookey and Kendall, 2007), or it may be associated with the impingement of slab material upon the CMB, resulting in high stresses and high-strain horizontal deformation accommodated in the dislocation creep regime (McNamara et al., 2002). The picture of LPO development in lowermost mantle minerals remains incomplete (e.g., Yamazaki and Karato, 2007), and this ambiguity also hampers the interpretation of anisotropy measurements in terms of mantle flow, although a few studies have attempted

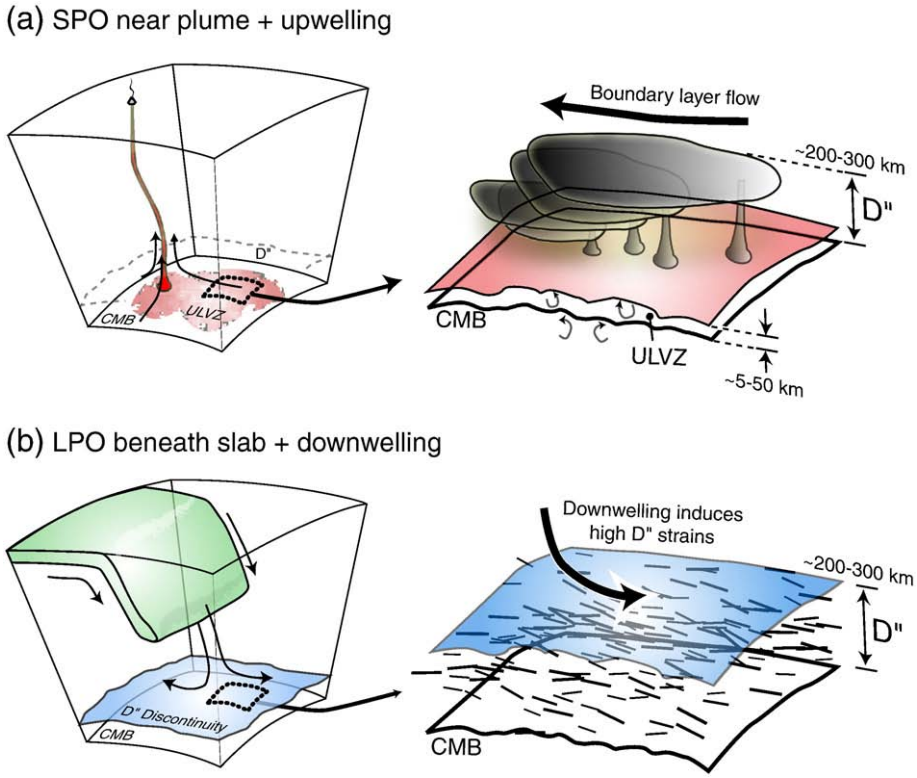

Fig. 9. Cartoon of possible mechanisms for D" anisotropy, after Moore et al. (2004). In the first scenario (top), partial melt associated with ultra-low velocity zones may occur throughout the D" volume if the melt is close to neutral buoyancy or if advection is fast compared to percolation velocities (Moore et al., 2004). The melt is aligned to produce SPO by horizontal shear flow above the CMB in the vicinity of a narrow upwelling. In the second scenario (bottom), a downgoing slab impinging upon the CMB induces high-stress, high-strain deformation in the dislocation creep regime, which induces the LPO of lowermost mantle minerals (cf. Fig. 1).

to reconcile the predictions from models of downgoing slabs above the CMB with observations of D" anisotropy (e.g., McNamara et al., 2002; Wenk et al., 2006; Merkel et al., 2007).

6. Outstanding problems and avenues for progress

Progress has been made over the past decades in characterizing the first-order anisotropy of the mantle and in understanding how to use those constraints to gain insight into mantle dynamics. Global geodynamic models that take into account density-driven flow and surface plate motions do a good job of matching observations of upper mantle anisotropy in the relatively simple tectonic setting of the ocean basins, suggesting that our basic understanding of the relationship between strain and anisotropy in the sub-oceanic upper mantle is apt. Upper mantle anisotropy in more complicated regions such as beneath continental interiors and in subduction systems has also been imaged. While our understanding of these regions remains incomplete, dense data sets that can be better interrogated for complex dynamics (e.g., the USArray component of the EarthScope project) are increasingly common. Evidence for anisotropy in deeper regions such as the transition zone and D" layer provides a tantalizing target for ongoing studies of the dynamics of the deep mantle. Here, we briefly discuss a few outstanding problems in the study of mantle anisotropy and exciting avenues for progress in the near future.

A longstanding puzzle in the study of upper mantle anisotropy has been the often-conflicting views of anisotropy provided by surface wave observations and shear wave splitting measurements. Surface and body waves sample on different length scales and depth dependence, and coverage is uneven in dissimilar ways. However, many studies have sought to reconcile surface wave models and splitting measurements by, for example, predicting shear wave splitting from surface wave models and comparing them to observations (Montagner et al., 2000). Often, these comparisons are not particularly successful for continental-scale models (e.g., Australia; Simons et al., 2002; Debayle et al., 2005) and while global models fit relatively well, the fit is notably poor in many regions (Wüstefeld et al., 2009). The natural way to address these discrepancies between surface and body wave azimuthal anisotropy is to take layered anisotropy into account (e.g., Silver and Savage, 1994; Saltzer et al., 2000) when computing equivalent shear wave splitting, and the incorporation of more accurate theory is likely to improve the fit. From an observational point of view, a more detailed characterization of shear wave splitting allowing for 3D structure at depth will also be helpful. Recent theoretical advances for shear wave splitting tomography (e.g., Chevrot et al., 2004; Chevrot, 2006; Abt and Fischer, 2008; Long et al., 2008) have made it possible to invert splitting measurements for anisotropy at depth, although such inversions require data from dense arrays. Further developments, both theoretical and practical, are likely to make the tomographic inversion of splitting measurements more common and will also pave the way for the joint inversion of surface wave and splitting data for anisotropic models (e.g., Marone and Romanowicz, 2007). We view progress in the 3D imaging of anisotropic structure, including shear wave splitting tomography and ambient noise tomography of crustal and uppermost mantle anisotropy (e.g., Moschetti et al., 2010), as extremely important for advancing our understanding of complex dynamic processes at depth.

Further progress in 3D imaging of upper mantle anisotropy also will help to resolve outstanding problems related to the dynamics of subduction systems and other complex tectonic settings, the nature of the asthenosphere, and the evolution of continental interiors. A more thorough characterization of anisotropy in subduction systems can be

aided by the deployment of dense arrays in subduction zones, and by thoroughly investigating complex splitting patterns, including, for example, frequency-dependent splitting (e.g., Greve and Savage, 2009). On the modeling side, a better understanding of the relationship between rheological and compositional complexities to slab-related 3D flow is also important. While some models have demonstrated that trench rollback can induce trench-parallel mantle flow beneath the slab (e.g., Fig. 8), the full parameter space for these types of models remains to be explored in more regionally realistic, and dynamically evolving settings. While we have focused on subduction systems in this review, improved characterization of anisotropy in other complex tectonic settings such as mantle upwellings (e.g., Walker et al., 2005), mid-ocean ridges (e.g., Wolfe and Solomon, 1998), continental rifts (e.g., Kendall et al., 2004), and vicinity of faults (e.g., Savage et al., 2004) should also yield powerful insight into the dynamics of these systems.

The nature of the transition between the thermo-chemical lithosphere and the sub-oceanic and sub-continental asthenosphere is another current study area. In oceanic domains, further analysis of a range of seismological data and geodynamic models, in conjunction with other efforts such as electro-magnetic surveying and magneto-telluric studies, will shed light on the distribution of volatiles and melts, as well as the rheology of the asthenosphere. Dynamic questions to be further addressed include the role of small-scale convection and the interactions of plate- with plume- and keel-scale flow. The evolution and dynamics of continental interiors are other issues that are currently being addressed (e.g., Fouch and Rondenay, 2006). A more thorough characterization of anisotropy in the continental upper mantle will increase our understanding of, for example, the vertical coherence of lithospheric deformation, the depth extent of localization along faults, and the formation of cratons by processes such as slab stacking. As with other tectonic settings, a better understanding of the depth distribution of anisotropy is crucial in order to properly separate the signal from frozen lithospheric anisotropy, which records previous tectonic stages, and asthenospheric anisotropy due to contemporary mantle flow. Further improvements in the resolution of surface wave tomographic models that incorporate azimuthal anisotropy, facilitated by the availability of dense array data, is likely to yield additional insight into this depth distribution (e.g., Deschamps et al., 2008; Zhang et al., 2009; Lin et al., in review).

Lastly, anisotropy in the D" region is an exciting frontier. We have not yet reached the point of being able to reliably relate the geometry of anisotropy to mantle flow in D", as we have for the upper mantle. However, this should be a tractable problem, and we expect future insights into the dynamics of the deep mantle to result from studies of D" anisotropy. Progress on understanding the geometry of deep anisotropy will come, again, from array type studies and from combining different types of phases that sample the same region in different geometries, which is a promising but challenging prospect. If a relationship between strain and anisotropy at D" conditions can reliably be established in the laboratory and by theoretical simulation, then observations of D" anisotropy could be used to map mantle flow. Future comparisons of predictions from global flow models with observations of D" anisotropy will likely lead to insights about the rheology of the lowermost mantle, the extent of partial melting, the nature of chemical heterogeneity, and the effect of large-scale structures such as thermo-chemical piles (e.g., Garnero and McNamara, 2008) on lowermost mantle dynamics.

7. Summary

Seismic anisotropy is found throughout the solid Earth and observations of anisotropy in the mantle can provide constraints on a range of dynamical questions. Those include first-order pattern of mantle convection, nature of the lithosphere–asthenosphere transition, slab dynamics, continental evolution, lowermost mantle dynamics, and core–mantle interactions. Quantitative geodynamic studies of upper mantle circulation have been remarkably successful in explaining a range of large-scale azimuthal and radial anisotropy features. This implies that our understanding of the formation of mantle anisotropy in convective flow, and associated forward modeling approaches, may be correct to first order. Anisotropy can then be used to answer more intricate questions by testing deviations from geodynamic "reference" models, for example as to the role of trench rollback, the appropriate mantle rheology, the hydration state of the upper mantle, and the net rotations of the lithosphere.

There are large remaining uncertainties involving geodynamic forward modeling, mineral physics constraints, and seismological imaging, and the resulting non-uniqueness of interpretation becomes more apparent for regional applications. The ongoing debate about the extent of anisotropic variability underneath old continental crust is one example where further progress on the imaging side, along with better constraints from mineral physics, is still needed to arrive at a more complete understanding of continental evolution. We expect to see great progress over the next 10 years thanks to ongoing efforts in the community that include more sophisticated geodynamic forward modeling, array-type seismological deployments such as EarthScope USArray, 3D imaging theory improvements, and expanded laboratory studies on anisotropy formation.

Acknowledgements

We thank Ed Garnero for permission to reproduce Fig. 9, Shun Karato for permission to reproduce the olivine pole figures shown in Fig. 3, and Mark Behn, Clint Conrad, and Shun Karato for helpful comments on a draft of this manuscript. We are grateful for reviews from Karen Fischer and three anonymous reviewers that helped to improve the paper. MDL acknowledges support from NSF grant EAR-0911286 and from Yale University, and TWB acknowledges support from NSF grant EAR-0643365.

We dedicate this paper to the memory of the late Paul Silver, whose contributions to the study of seismic anisotropy were enormous and who was an inspiration to many. It was Paul's question about "what mantle flow actually looks like beneath western North America" that sent TWB down the anisotropy rabbit hole, and MDL remembers Paul as a wonderful mentor and collaborator who was wildly enthusiastic about his science and tireless in his support of junior colleagues.

References

Abt, D.L., Fischer, K.M., 2008. Resolving three-dimensional anisotropic structure with shear-wave splitting tomography. Geophys. J. Int. 173, 859–886.

Abt, D.L., Fischer, K.M., Abers, G.A., Protti, M., Gonzalez, V., Strauch, W., 2010. Constraints on upper mantle anisotropy surrounding the Cocos slab from SK(K)S splitting. J. Geophys. Res. 115, B06316. doi:10.1029/2009JB006710.

Abt, D.L., Fischer, K.M., Abers, G.A., Strauch, W., Protti, J.M., Gonzalez, V., 2009. Shear-wave anisotropy beneath Nicaragua and Costa Rica: implications for flow in the mantle wedge. Geochem. Geophys. Geosyst. Q05S15. doi:10.1029/2009GC002375.

Becker, T.W., 2008. Azimuthal seismic anisotropy constrains net rotation of the lithosphere. Geophys. Res. Lett. 35, L05303. doi:10.1029/2008GL033946.

Becker, T.W., Browaeys, J.T., Jordan, T.H., 2007. Stochastic analysis of shear wave splitting length scales. Earth Planet. Sci. Lett. 259, 526–540.

Becker, T.W., Chevrot, S., Schulte-Pelkum, V., Blackman, D.K., 2006. Statistical properties of seismic anisotropy predicted by upper mantle geodynamic models. J. Geophys. Res. 111, B08309. doi:10.1029/2005JB004095.

Becker, T.W., Faccenna, C., 2009. A review of the role of subduction dynamics for regional and global plate motions. In: Lallemand, S., Funiciello, F. (Eds.), Subduction Zone Geodynamics. Springer, pp. 3–34.

Becker, T.W., Kellogg, J.B., Ekström, G., O'Connell, R.J., 2003. Comparison of azimuthal seismic anisotropy from surface waves and finite-strain from global mantle-circulation models. Geophys. J. Int. 155, 696–714.

Becker, T.W., Kustowski, B., Ekström, G., 2008. Radial seismic anisotropy as a constraint for upper mantle rheology. Earth Planet. Sci. Lett. 267, 213–237.

Beghein, C., Trampert, J., 2003. Robust normal mode constraints in inner-core anisotropy from model space search. Science 299, 552–555.

Behn, M.D., Conrad, C.P., Silver, P.G., 2004. Detection of upper mantle flow associated with the African superplume. Earth Planet. Sci. Lett. 224, 259–274.
Behn, M.D., Hirth, G., Kelemen, P.B., 2007. Lower crustal foundering as a mechanism for trench parallel anisotropy. Science 317, 108–111.
Ben Ismaïl, W., Mainprice, D., 1998. An olivine fabric database: an overview of upper mantle fabrics and seismic anisotropy. Tectonophysics 296, 145–157.
Bezacier, L., Reynard, B., Bass, J.D., Sanchez-Valle, C., van de Moortèle, B., 2010. Elasticity of antigorite, seismic detection of serpentinites, and anisotropy in subduction zones. Earth Planet. Sci. Lett. 289, 198–208.
Billen, M.I., 2008. Modeling the dynamics of subducting slabs. Annu. Rev. Earth Planet. Sci. 36, 325–356.
Blackman, D.K., Wenk, H.-R., Kendall, J.-M., 2002. Seismic anisotropy of the upper mantle: 1. Factors that affect mineral texture and effective elastic properties. Geochem. Geophys. Geosyst. 3, 8601. doi:10.1029/2001GC000248.
Bokelmann, G.H.R., 2002. Convection-driven motion of the North American craton: evidence from P-wave anisotropy. Geophys. J. Int. 148, 278–287.
Boschi, L., Dziewonski, A.M., 2000. Whole Earth tomography from delay times of P, PcP, PKP phases: lateral heterogeneities in the outer core, or radial anisotropy in the mantle? J. Geophys. Res. 105, 25,567–25,594.
Bystricky, M., Kunze, K., Burlini, L., Burg, J.-P., 2000. High shear strain of olivine aggregrates: rheological and seismic consequences. Science 290, 1564–1567.
Cagnioncle, A.M., Parmentier, E.M., Elkins-Tanton, L.T., 2007. The effect of solid flow above a subducting slab on water distribution and melting at convergent plate boundaries. J. Geophys. Res. 112, B09402. doi:10.1029/2007JB004934.
Castelnau, O., Blackman, D.K., Becker, T.W., 2009. Numerical simulations of texture development and associated rheological anisotropy in regions of complex mantle flow. Geophys. Res. Lett. 36, L12304. doi:10.1029/2009GL038027.
Chastel, Y.B., Dawson, P.R., Wenk, H.R., Bennett, K., 1993. Anisotropic convection with implications for the upper mantle. J. Geophys. Res. 98, 17,757–17,771.
Chevrot, S., 2000. Multichannel analysis of shear wave splitting. J. Geophys. Res. 105, 21,579–21,590.
Chevrot, S., Favier, N., Komatitsch, D., 2004. Shear wave splitting in three-dimensional anisotropic media. Geophys. J. Int. 159, 711–720.
Chevrot, S., 2006. Finite-frequency vectorial tomography: a new method for high-resolution imaging of upper mantle anisotropy. Geophys. J. Int. 165, 641–657.
Christensen, U.R., 1987. Some geodynamical effects of anisotropic viscosity. Geophys. J. R. Astron. Soc. 91, 711–736.
Clitheroe, G., van der Hilst, R.D., 1998. Complex anisotropy in the Australian lithosphere from shear-wave splitting in broad-band SKS records. In: Braun, J., et al. (Ed.), Structure and Evolution of the Australian Continent. American Geophysical Union, pp. 73–78.
Conrad, C.P., Behn, M.D., 2010. Constraints on lithosphere net rotation and asthenospheric viscosity from global mantle flow models and seismic anisotropy. Geochem. Geophys. Geosyst. 11, Q05W05. doi:10.1029/2009GC002970.
Conrad, C.P., Behn, M.D., Silver, P.G., 2007. Global mantle flow and the development of seismic anisotropy: differences between the oceanic and continental upper mantle. J. Geophys. Res. 112, B07317. doi:10.1029/2006JB004608.
Crampin, S., 1981. A review of wave motion in anisotropic and cracked elastic-media. Wave Motion 3, 343–391.
Crampin, S., Chastin, S., 2003. A review of shear wave splitting in the crack-critical crust. Geophys. J. Int. 155, 221–240.
Debayle, E., Kennett, B., Priestly, K., 2005. Global azimuthal seismic anisotropy and the unusual plate-motion deformation of Australia. Nature 433, 509–512.
Deschamps, F., Lebedev, S., Meier, T., Trampert, J., 2008. Stratified seismic anisotropy reveals past and present deformation beneath the east-central United States. Earth Planet. Sci. Lett. 274, 489–498.
Dziewonski, A.M., Anderson, D.L., 1981. Preliminary reference Earth model. Phys. Earth Planet. Inter. 25, 297–356.
England, P., Wilkins, C., 2004. A simple analytical approximation to the temperature structure in subduction zones. Geophys. J. Int. 159, 1138–1154.
Faccenda, M., Burlini, L., Gerya, T.V., Mainprice, D., 2008. Fault-induced seismic anisotropy by hydration in subducting oceanic plates. Nature 455, 1097–1100.
Ferreira, A.M.G., Woodhouse, J.H., Visser, K., Trampert, J., 2010. On the robustness of global radially anisotropic surface wave tomography. J. Geophys. Res. 115, B04313. doi:10.1029/2009JB006716.
Fischer, K.M., Parmentier, E.M., Stine, A.R., Wolf, E.R., 2000. Modeling anisotropy and plate-driven flow in the Tonga subduction zone back arc. J. Geophys. Res. 105, 16,181–16,191.
Fischer, K.M., Wiens, D.A., 1996. The depth distribution of mantle anisotropy beneath the Tonga subduction zone. Earth Planet. Sci. Lett. 142, 253–260.
Forsyth, D.W., 1975. The early structural evolution and anisotropy of the oceanic upper mantle. Geophys. J. R. Astron. Soc. 43, 103–162.
Forte, A.M., 2007. Constraints on seismic models from other disciplines—implications for mantle dynamics and composition. In: Schubert, G. (Ed.), Treatise on Geophysics v. 1, pp. 805–858.
Fouch, M.J., 2006. Upper mantle anisotropy database. Accessed in 06/2006, http://geophysics.asu.edu/anisotropy/upper/.
Fouch, M.J., Fischer, K.M., Parmentier, E.M., Wysession, M.E., Clarke, T.J., 2000. Shear wave splitting, continental keels, and patterns of mantle flow. J. Geophys. Res. 105, 6255–6275.
Fouch, M.J., Rondenay, S., 2006. Seismic anisotropy beneath stable continental interiors. Phys. Earth Planet. Inter. 158, 292–320.
Fouch, M.J., Silver, P.G., Bell, D.R., Lee, J.N., 2004. Small-scale variations in seismic anisotropy near Kimberley, South Africa. Geophys. J. Int. 157, 764–774.
Funiciello, F., Moroni, M., Piromallo, C., Faccenna, C., Cenedese, A., Bui, H.A., 2006. Mapping mantle flow during retreating subduction: laboratory models analyzed by feature tracking. J. Geophys. Res. 111, B03402. doi:10.1029/2005JB003792.
Gaboret, C., Forte, A.M., Montagner, J.-P., 2003. The unique dynamics of the Pacific Hemisphere mantle and its signature on seismic anisotropy. Earth Planet. Sci. Lett. 208, 219–233.
Garnero, E.J., Maupin, V., Lay, T., Fouch, M.J., 2004. Variable azimuthal anisotropy in Earth's lowermost mantle. Science 306, 259–261.
Garnero, E.J., McNamara, A.K., 2008. Structure and dynamics of the Earth's lower mantle. Science 320, 626–628.
Gouillou-Frottier, L., Buttles, J., Olson, P., 1995. Laboratory experiments on the structure of subducted lithosphere. Earth Planet. Sci. Lett. 133, 19–34.
Greve, S.M., Savage, M.K., 2009. Modelling seismic anisotropy variations across the Hikurangi subduction margin, New Zealand. Earth Planet. Sci. Lett. 285, 16–26.
Gripp, A.E., Gordon, R.G., 2002. Young tracks of hot spots and current plate velocities. Geophys. J. Int. 150, 321–361.
Grove, T.L., Till, C.B., Lev, E., Chatterjee, N., Médard, E., 2009. Kinematic variables and water transport control the formation and location of arc volcanoes. Nature 459, 694–697.
Hager, B.H., 1984. Subducted slabs and the geoid: constraints on mantle rheology and flow. J. Geophys. Res. 89, 6003–6015.
Hager, B.H., Clayton, R.W., 1989. Constraints on the structure of mantle convection using seismic observations, flow models, and the geoid. In: Peltier, W.R. (Ed.), Mantle convection: plate tectonics and global dynamics. Gordon and Breach, New York, NY, pp. 657–763.
Hager, B.H., O'Connell, R.J., 1981. A simple global model of plate dynamics and mantle convection. J. Geophys. Res. 86, 4843–4867.
Hall, C., Fischer, K.M., Parmentier, E.M., Blackman, D.K., 2000. The influence of plate motions on three-dimensional back arc mantle flow and shear wave splitting. J. Geophys. Res. 105, 28,009–28,033.
Heintz, M., Kennett, B.L.N., 2005. Continental scale shear wave splitting analysis: investigation of seismic anisotropy underneath the Australian continent. Earth Planet. Sci. Lett. 236, 106–119.
Heintz, M., Kennett, B.L.N., 2006. The apparently isotropic Australian upper mantle. Geophys. Res. Lett. 33, L15319. doi:10.1029/2006GL026401.
Hoernle, K., Abt, D.L., Fischer, K.M., Nichols, H., Hauff, F., Abers, G.A., van der Bogaard, P., Heydolph, K., Alvarado, G., Protti, M., Strauch, W., 2008. Geochemical and geophysical evidence for arc-parallel flow in the mantle wedge beneath Costa Rica and Nicaragua. Nature 451, 1094–1098.
Jung, H., Jiang, Z., Katayama, I., Hiraga, T., Karato, S., 2006. The effects of water and stress on lattice preferred orientation in olivine. Tectonophysics 421, 1–22.
Jung, H., Karato, S., 2001. Water-induced fabric transitions in olivine. Science 293, 1460–1463.
Jung, H., Mo, W., Green, H.W., 2009. Upper mantle seismic anisotropy resulting from pressure-induced slip transition in olivine. Nat. Geosci. 2, 73–77.
Kaminski, É., 2002. The influence of water on the development of lattice preferred orientation in olivine aggregates. Geophys. Res. Lett. 29, 1576. doi:10.1029/2002GL014710.
Kaminski, É., Ribe, N.M., 2001. A kinematic model for recrystallization and texture development in olivine polycrystals. Earth Planet. Sci. Lett. 189, 253–267.
Kaminski, É., Ribe, N.M., 2002. Timescales for the evolution of seismic anisotropy in mantle flow. Geochem. Geophys. Geosyst. 3, 1051. doi:10.1029/2001GC000222.
Kaminski, É., Ribe, N.M., Browaeys, J.T., 2004. D-Rex, a program for calculation of seismic anisotropy due to crystal lattice preferred orientation in the convective upper mantle. Geophys. J. Int. 158, 744–752.
Karato, S., 1995. Effects of water on seismic wave velocities in the upper mantle. Proc. Jpn Acad. 71, 61–66.
Karato, S., 1998. Some remarks on the origin of seismic anisotropy in the D" layer. Earth Planets Space 50, 1019–1028.
Karato, S., 2008. Insight into the plume-upper mantle interaction inferred from the central Pacific geophysical anomalies. Earth Planet. Sci. Lett. 274, 234–240.
Karato, S., Jung, H., Katayama, I., Skemer, P., 2008. Geodynamic significance of seismic anisotropy of the upper mantle: new insights from laboratory studies. Annu. Rev. Earth Planet. Sci. 36, 59–95.
Karato, S., Zhang, S., Wenk, H.-R., 1995. Superplasticity in Earth's lower mantle: evidence from seismic anisotropy and rock physics. Science 270, 458–461.
Katayama, I., Hirauchi, K., Michibayashi, K., Ando, J., 2009. Trench-parallel anisotropy produced by serpentine deformation in the hydrated mantle wedge. Nature 461, 1114–1117.
Kendall, J.M., Silver, P.G., 1998. Investigating causes of D" anisotropy. In: Gurnis, M., et al. (Ed.), The Core-Mantle Boundary Region. American Geophysical Union, pp. 97–118.
Kendall, J.-M., Stuart, G.W., Ebinger, C.J., Bastow, I.D., Keir, D., 2004. Magma-assisted rifting in Ethiopia. Nature 433, 146–148.
Kincaid, C., Griffiths, R.W., 2003. Laboratory models of the thermal evolution of the mantle during rollback subduction. Nature 425, 58–62.
Kneller, E.A., van Keken, P.E., 2008. The effects of three-dimensional slab geometry on deformation in the mantle wedge: implications for shear wave anisotropy. Geochem. Geophys. Geosyst. 9, Q01003. doi:10.1029/2007GC001677.
Kneller, E.A., Long, M.D., van Keken, P.E., 2008. Olivine fabric transitions and shear-wave anisotropy in the Ryukyu subduction system. Earth Planet. Sci. Lett. 268, 268–282.
Knoll, M., Tommasi, A., Logé, R., Signorelli, J., 2009. A multiscale approach to model the anisotropic deformation of lithospheric plates. Geochem. Geophys. Geosyst. 10, Q08009. doi:10.1029/2009GC002423.
Kohlstedt, D.L., 2007. Constitutive equations, rheological behavior, and viscosity of rocks. In: Schubert, G. (Ed.), Treatise on Geophysics v. 2, pp. 389–417.
Kreemer, C., 2009. Absolute plate motions constrained by shear wave splitting orientations with implications for hot spot motions and mantle flow. J. Geophys. Res. 114, B10405. doi:10.1029/2009JB006416.

Kustowski, B., Ekström, G., Dziewonski, A.M., 2008. Anisotropic shear wave velocity of the Earth's mantle: a global model. J. Geophys. Res. 113. doi:10.1029/2007JB005169.
Lassak, T.M., Fouch, M.J., Hall, C.E., Kaminski, É., 2006. Seismic characterization of mantle flow in subduction systems: can we resolve a hydrated mantle wedge? Earth Planet. Sci. Lett. 243, 632–649.
Lebedev, S., van der Hilst, R.D., 2008. Global upper-mantle tomography with the automated multimode inversion of surface and S-wave forms. Geophys. J. Int. 173, 505–518.
Lev, E., Hager, B.H., 2008a. Rayleigh–Taylor instabilities with anisotropic lithospheric viscosity. Geophys. J. Int. 173, 806–814.
Lev, E., Hager, B.H., 2008b. Prediction of anisotropy from flow models: a comparison of three methods. Geochem. Geophys. Geosyst. 9, Q07014. doi:10.1029/2008GC002032.
Levin, V., Droznin, D., Park, J., Gordeev, E., 2004. Detailed mapping of seismic anisotropy with local shear waves in southeastern Kamchatka. Geophys. J. Int. 158, 1009–1023.
Levin, V., Park, J., 1998. P-SH conversions in layered media with hexagonally symmetric anisotropy: a cookbook. Pure Appl. Geophys. 151, 669–697.
Lin, F-C., Ritzwoller, M.H., Yang, Y., Moschetti, M.P. Fouch, M.J., 2010. The stratification of seismic azimuthal anisotropy in the western US. Nature, in review.
Long, M.D., 2009. Complex anisotropy in D" beneath the eastern Pacific from SKS–SKKS splitting discrepancies. Earth Planet. Sci. Lett. 283, 181–189.
Long, M.D., de Hoop, M.V., van der Hilst, R.D., 2008. Wave-equation shear wave splitting tomography. Geophys. J. Int. 172, 311–330.
Long, M.D., Silver, P.G., 2008. The subduction zone flow field from seismic anisotropy: a global view. Science 319, 315–318.
Long, M.D., Silver, P.G., 2009a. Shear wave splitting and mantle anisotropy: measurements, interpretations, and new directions. Surv. Geophys. 30, 407–461.
Long, M.D., Silver, P.G., 2009b. Mantle flow in subduction systems: the subslab flow field and implications for mantle dynamics. J. Geophys. Res. 114, B10312. doi:10.1029/ 2008JB006200.
Long, M.D., van der Hilst, R.D., 2006. Shear wave splitting from local events beneath the Ryukyu arc: trench-parallel anisotropy in the mantle wedge. Phys. Earth Planet. Inter. 155, 300–312.
Long, M.D., Xiao, X., Jiang, Z., Evans, B., Karato, S., 2006. Lattice preferred orientation in deformed polycrystalline (Mg, FeO) and implications for seismic anisotropy in D". Phys. Earth Planet. Inter. 156, 75–88.
Mainprice, D., 2007. Seismic anisotropy of the deep Earth from a mineral and rock physics perspective. In: Schubert, G. (Ed.), Treatise on Geophysics v. 2, pp. 437–492.
Mainprice, D., Nicolas, A., 1989. Development of shape and lattice preferred orientations: application to the seismic anisotropy of the lower crust. J. Struct. Geol. 11, 175–189.
Mainprice, D., Tommasi, A., Couvy, H., Cordier, P., Frost, D.J., 2005. Pressure sensitivity of olivine slip systems: implications for the interpretation of seismic anisotropy of the Earth's upper mantle. Nature 433, 731–733.
Marone, F., Romanowicz, 2007. The depth distribution of azimuthal anisotropy in the continental upper mantle. Nature 447, 198–201.
McKenzie, D., 1979. Finite deformation during fluid flow. Geophys. J. R. Astron. Soc. 58, 689–715.
McNamara, A.K., van Keken, P.E., Karato, S., 2002. Development of anisotropic structure by solid-state convection in the Earth's lower mantle. Nature 416, 310–314.
Meade, C., Silver, P.G., Kaneshima, S., 1995. Laboratory and seismological observations of lower mantle isotropy. Geophys. Res. Lett. 22, 1293–1296.
Mehl, L., Hacker, B.R., Hirth, G., Kelemen, P.B., 2003. Arc-parallel flow within the mantle wedge: evidence from the accreted Talkeetna arc, south central Alaska. J. Geophys. Res. 108, B8, 2375. doi:10.1029/2002JB002233.
Meissner, R., Rabbel, W., Kern, H., 2006. Seismic lamination and anisotropy of the lower continental crust. Tectonophysics 416, 81–99.
Merkel, S., Kubo, A., Miyagi, L., Speziale, S., Duffy, T.S., Mao, H.-K., Wenk, H.-R., 2006. Plastic deformation in MgGeO3 post-perovskite at lower mantle pressures. Science 311, 644–646.
Merkel, S., McNamara, A.K., Kubo, A., Speziale, S., Miyagi, L., Meng, Y., Duffy, T.S., Wenk, H.-R., 2007. Deformation of (Mg, Fe)SiO3 post-perovskite and D" anisotropy. Science 316, 1729–1732.
Mihalffy, P., Steinberger, B., Schmeling, H., 2008. The effect of the large-scale mantle flow field on the Iceland hotspot track. Tectonophysics 447, 53–65.
Mizukami, T., Wallis, S.R., Yamamoto, J., 2004. Natural examples of olivine lattice preferred orientation patterns with a flow-normal a-axis minimum. Nature 427, 432–436.
Montagner, J.-P., 2007. Deep Earth structure—upper mantle structure from isotropic and anisotropic elastic tomography. In: Schubert, G. (Ed.), Treatise on Geophysics v. 1, pp. 559–589.
Montagner, J.-P., Nataf, H.-C., 1986. A simple method for inverting the azimuthal anisotropy of surface waves. J. Geophys. Res. 91, 511–520.
Montagner, J.-P., Griot-Pommera, D.A., Lavé, J., 2000. How to relate body wave and surface wave anisotropy? J. Geophys. Res. 105, 19,015–19,027.
Montagner, J.-P., Tanimoto, T., 1991. Global upper mantle tomography of seismic velocities and anisotropies. J. Geophys. Res. 96, 20337–20351.
Moore, M.M., Garnero, E.J., Lay, T., Williams, Q., 2004. Shear wave splitting and waveform complexity for lowermost mantle structures with low-velocity lamellae and transverse isotropy. J. Geophys. Res. 103, B023019. doi:10.1029/2003JB002546.
Moschetti, M.P., Ritzwoller, M.H., Lin, F., Yang, Y., 2010. Seismic evidence for widespread western-US deep-crustal deformation caused by extension. Nature 464, 885–889.
Nakajima, J., Hasegawa, A., 2004. Shear-wave polarization anisotropy and subduction-induced flow in the mantle wedge of northern Japan. Earth Planet. Sci. Lett. 225, 365–377.
Nataf, H.-C., Nakanishi, I., Anderson, D.L., 1984. Anisotropy and shear velocity heterogeneity in the upper mantle. Geophys. Res. Lett. 11, 109–112.
Nicolas, A., Bouches, J.L., Boudier, F., Mercier, J.-C.C., 1971. Textures, structures and fabrics due to solid state flow in some European lherzolites. Tectonophysics 12, 55–86.
Panning, M., Romanowicz, B., 2006. A three-dimensional radially anisotropic model of shear velocity in the whole mantle. Geophys. J. Int. 167, 361–379.
Peacock, S., 2003. Thermal structure and metamorphic evoluation of subducting slabs. In: Eiler, J. (Ed.), Inside the Subduction Factory. American Geophysical Union, pp. 7–22.
Piromallo, C., Becker, T.W., Funiciello, F., Faccenna, C., 2006. Three-dimensional instantaneous mantle flow induced by subduction. Geophys. Res. Lett. 33, L08304. doi:10.1029/2005GL025390.
Plomerová, J., Sileny, J., Babuska, V., 1996. Joint interpretation of upper-mantle anisotropy based on teleseismic P-travel time delays and inversion of shear-wave splitting paramters. Phys. Earth Planet. Inter. 95, 293–309.
Pouilloux, L., Kaminski, E., Labrosse, S., 2007. Anisotropic rheology of a cubic medium and implications for geological materials. Geophys. J. Int. 170, 876–885.
Pozgay, S.H., Wiens, D.A., Conder, J.A., Shiobara, H., Sugioka, H., 2007. Complex mantle flow in the Mariana subduction system: evidence from shear wave splitting. Geophys. J. Int. 170, 371–386.
Ricard, Y., Vigny, C., 1989. Mantle dynamics with induced plate tectonics. J. Geophys. Res. 94, 17,543–17,559.
Rieger, D.M., Park, J., 2010. USArray observations of quasi-Love surface wave scattering: Orienting anisotropy in the Cascadia plate boundary. J. Geophys. Res. 115, B05306. doi:10.1029/2009JB006754.
Ritsema, J., 2000. Evidence for shear velocity anisotropy in the lowermost mantle beneath the Indian Ocean. Geophys. Res. Lett. 27, 1041–1044.
Russo, R.M., 2009. Subducted oceanic asthenosphere and upper mantle flow beneath the Juan de Fuca slab. Lithosphere 1, 195–205.
Russo, R.M., Silver, P.G., 1994. Trench-parallel flow beneath the Nazca plate from seismic anisotropy. Science 263, 1105–1111.
Saltzer, R.L., Gaherty, J.B., Jordan, T.H., 2000. How are vertical shear wave splitting measurements affected by variations in the orientation of azimuthal anisotropy with depth? Geophys. J. Int. 141, 374–390.
Savage, M.K., 1999. Seismic anisotropy and mantle deformation: what have we learned from shear wave splitting? Rev. Geophys. 37, 65–106.
Savage, M.K., Fischer, K.M., Hall, C.E., 2004. Strain modeling, seismic anisotropy and coupling at strike-slip boundaries: applications in New Zealand and the San Andreas fault. In: Grocott, J., et al. (Ed.), Vertical coupling and decoupling in the lithosphere. Geological Society of London Special Publications, pp. 9–40.
Schellart, W.P., Freeman, J., Stegman, D.R., Moresi, L., May, D., 2007. Evolution and diversity of subduction zones controlled by slab width. Nature 446, 308–311.
Schulte-Pelkum, V., Masters, G., Shearer, P.M., 2001. Upper mantle anisotropy from long-period P polarization. J. Geophys. Res. 106 (B10), 21,917–21,934.
Silver, P.G., 1996. Seismic anisotropy beneath the continents: probing the depths of geology. Annu. Rev. Earth Planet. Sci. 24, 385–432.
Silver, P.G., Chan, W.W., 1991. Shear wave splitting and subcontinental mantle deformation. J. Geophys. Res. 96, 16,429–16,454.
Silver, P.G., Savage, M.K., 1994. The interpretation of shear-wave splitting parameters in the presence of two anisotropic layers. Geophys. J. Int. 119, 949–963.
Simmons, N.A., Forte, A.M., Grand, S.P., 2009. Joint seismic, geodynamic and mineral physics constraints on three-dimensional mantle heterogeneity: implications for the relative importance of thermal versus compositional heterogeneity. Geophys. J. Int. 177, 1284–1304.
Simons, F.J., van der Hilst, R.D., Montagner, J.-P., Zielhuis, A., 2002. Multimode Rayleigh wave inversion for heterogeneity and azimuthal anisotropy of the Australian upper mantle. Geophys. J. Int. 151, 738–754.
Skemer, P., Katayama, I., Karato, S.-i., 2006. Deformation fabrics of the Cima di Gagnone Peridotite Massif, Central Alps, Switzerland: evidence of deformation at low temperatures in the presence of water. Contrib. Mineral. Petrol. 152, 43–51.
Smith, G.P., Ekström, G., 1999. A global study of Pn anisotropy beneath continents. J. Geophys. Res. 104 (B1), 963–980.
Smith, G.P., Wiens, D.A., Fischer, K.M., Dorman, L.M., Webb, S.C., Hildebrand, J.A., 2001. A complex pattern of mantle flow in the Lau Backarc. Science 292, 713–716.
Souriau, A., 2007. The Earth's core. In: Schubert, G. (Ed.), Treatise on Geophysics v. 1, pp. 655–693.
Stegman, D.R., Freeman, J., Schellart, W.P., Moresi, L.N., May, D.A., 2006. Influence of trench width on subduction hinge retreat rates in 3-D models of slab rollback. Geochem. Geophys. Geosyst. 7, Q03012. doi:10.1029/2005GC001056.
Tan, E., Choi, E., Thoutireddy, P., Gurnis, M., Aivazis, M., 2007. GeoFramework: Coupling multiple models of mantle convection within a computational framework. Geochem. Geophys. Geosyst. 7, Q06001. doi:10.1029/2005GC01155.
Tanimoto, T., Anderson, D.L., 1984. Mapping convection in the mantle. Geophys. Res. Lett. 11, 287–290.
Tommasi, A., Knoll, M., Vauchez, A., Signorelli, J.W., Thoraval, C., Logé, R., 2009. Structural reactivation in plate tectonics controlled by olivine crystal anisotropy. Nat. Geosci. 2, 423–427.
Trampert, J., van Heijst, H.J., 2002. Global azimuthal anisotropy in the transition zone. Science 296, 1297–1299.
Vinnik, L.P., Kind, R., Kosarev, G.L., Makeyeva, L., 1989. Azimuthal anisotropy in the lithosphere from observations of long-period S-waves. Geophys. J. Int. 99, 549–559.

Visser, K., Trampert, J., Lebedev, S., Kennett, B.L.N., 2008. Probability of radial anisotropy in the deep mantle. Earth Planet. Sci. Lett. 270, 241–250.
Walker, K.T., Bokelmann, G.H.R., Klemperer, S.L., Nyblade, A., Walker, K.T., Bokelmann, G.H.R., Klemperer, S.L., Nyblade, A., 2005. Shear-wave splitting around hotspots: evidence for upwelling-related mantle flow? In: Foulger, G., Foulger, G., et al. (Eds.), Plates, Plumes, & Paradigms. Geological Society of America, pp. 171–192.
Warren, J.M., Hirth, G., Kelemen, P.B., 2008. Evolution of lattice preferred orientation during simple shear in the mantle. Earth Planet. Sci. Lett. 272, 501–512.
Weiss, T., Siegesmund, S., Rabbel, W., Bohlen, T., Pohl, M., 1999. Seismic velocities and anisotropy of the lower continental crust: a review. Pure Appl. Geophys. 156, 97–122.
Wenk, H.-R., Bennett, K., Canova, G.R., Molinari, A., 1991. Modeling plastic deformation of peridotite with the self-consistent theory. J. Geophys. Res. 96, 8337–8349.
Wenk, H.-R., Speziale, S., McNamara, A.K., Garnero, E.J., 2006. Modeling lower mantle anisotropy development in a subducting slab. Earth Planet. Sci. Lett. 245, 302–314.
Wolfe, C.J., Solomon, S.C., 1998. Shear-wave splitting and implications for mantle flow beneath the MELT region of the East Pacific Rise. Science 280, 1230–1232.
Woodhouse, J., Giardini, D., Li, X.-D., 1986. Evidence for inner core anisotropy from free oscillations. Geophys. Res. Lett. 13, 1549–1552.
Wookey, J., Kendall, J.-M., 2004. Evidence of mid-mantle anisotropy from shear-wave splitting and the influence of shear-coupled P-waves. J. Geophys. Res. 109. doi:10.1029/ 2003JB002871.
Wookey, J., Kendall, J.-M., Rümpker, G., 2005. Lowermost mantle anisotropy beneath the North Pacific from differential S–ScS splitting. Geophys. J. Int. 161, 829–838.
Wookey, J., Kendall, J.M., 2007. Seismic anisotropy of post-perovskite and the lowermost mantle. In: Hirose, K., et al. (Ed.), Post-perovskite: the last mantle phase transition. American Geophysical Union, pp. 171–189.
Wüstefeld, A., Bokelmann, G., Barruol, G., Montagner, J.-P., 2009. Identifying global seismic anisotropy patterns by correlating shear-wave splitting and surface-wave data. Phys. Earth Planet. Inter. 176, 198–212.
Yamazaki, D., Karato, S., 2007. Lattice-preferred orientation of lower mantle materials and seismic anisotropy in the D" layer. In: Hirose, K., et al. (Ed.), Post-perovskite: the last mantle phase transition. American Geophysical Union, Washington, DC, pp. 69–78.
Yamazaki, D., Yoshino, T., Ohfuji, H., Ando, J., Yoneda, A., 2006. Origin of seismic anisotropy in the D" layer inferred from shear deformation experiments on post-perovskite phase. Earth Planet. Sci. Lett. 252, 372–378.
Zandt, G., Humphreys, E., 2008. Toroidal mantle flow through the western U.S. slab window. Geology 36, 295–298.
Zhang, S., Christensen, U., 1993. Some effects of lateral viscosity variations on geoid and surface velocities induced by density anomalies in the mantle. Geophys. J. Int. 114, 531–547.
Zhang, S., Karato, S., 1995. Lattice preferred orientation of olivine aggregates deformed in simple shear. Nature 415, 777–780.
Zhang, X., Paulssen, H., Lebedev, S., Meier, T., 2009. 3D shear velocity structure beneath the Gulf of California from Rayleigh wave dispersion. Earth Planet. Sci. Lett. 279, 255–262.
Zhong, S., Yuen, D.A., Moresi, L.N., 2007. Numerical methods for mantle convection. In: Schubert, G. (Ed.), Treatise on Geophysics v. 7, pp. 227–252.
Zhong, S., Zuber, M.T., Moresi, L., Gurnis, M., 2000. Role of temperature-dependent viscosity and surface plates in spherical shell models of mantle convection. J. Geophys. Res. 105, 11,063–11,082.

Maureen Long is an observational seismologist whose primary research interests lie in the domain of understanding the structure and dynamics of the Earth's mantle through studies of seismic anisotropy, with a focus on subduction systems. She received her Ph.D. from MIT in 2006 and is currently Assistant Professor of Geology and Geophysics at Yale University.

Thorsten Becker is a geophysicist whose main research interests are in geodynamics and seismology with focus on the interactions between mantle convection, geologic surface activity, and Earth evolution. He earned his Ph.D. from Harvard in 2002 and is currently Associate Professor of Earth Sciences at the University of Southern California.